Dissertation

Spin-Orbit Multiconfigurational Quantum Chemical Study on Nearly-Degenerate Low-Lying Electronic States of Heavy-Atom Contained Molecules

（スピン軌道相互作用を考慮した多配置波動関数による重原子系分子擬縮退電子状態の量子化学研究）

Yusuke KONDO

近藤有輔

Hokkaido University

Graduate School of Chemical Sciences and Engineering

Quantum Chemistry Laboratory

（北海道大学大学院総合化学院　量子化学研究室）

2018

Contents

1. General Introduction

1.1 The Schrödinger Equation

In quantum mechanics, theoretical foundation for electrons, atoms, and molecules is the Schrödinger equation [1]. To solve the electronic Schrödinger equation without parameters from experiments, *ab initio* quantum chemistry methods have advanced for 60 years, and nowadays quantum chemistry calculations have become an essential approach to interpret and understand the chemical phenomena from a microscopic viewpoint.

1.2 Wavefunction Theory vs. Density Functional Theory

There are two different approaches to treat an electronic structure: wavefunction theory and density functional theory (DFT). DFT is based on the Hohenberg-Kohn theorem [2] that the electronic ground-state energy for a given atomic system is uniquely determined by the electron density in a three-dimensional space. It is important to recognize that nobody knows the exact functionals for correlation and exchange energies. The applications of the DFT method are increasing more and more due to a simple input for a calculation and good agreement with experimental data, but there is no assurance that the solution of the DFT agrees with the solution of the Schrödinger equation. In this dissertation, I employ *ab initio* wave function theory throughout.

1.3 Large-Scale Quantum Chemical Approach

There are two directions in theoretical development of the electronic structure theory: large-scale and complexity. In a direction to a large-scale system, a drastic speedup in

computer technology in last three decades has brought a motivation to develop a linear-scaling methodology in *ab initio* wavefunction theory and density functional theory (DFT). Recently, sophisticated approaches such as fragment molecular orbital (FMO) method [3] and divide & conquer (DC) method [4] have been developed, and the number of applications to large-scale systems such as proteins has increased. A significant idea to treat a large-scale system is a combined approach of quantum mechanics and molecular mechanics (QM/MM) [5] such as ONIOM by Morokuma [6]. The Nobel prize in Chemistry in 2013 was awarded to Karplus, Levitt, and Warshel who initially proposed the idea of QM/MM approach for the development of multiscale models of complex chemical systems.

1.4 The Hartree-Fock Method and Electron Correlation

Another direction, the complexity in the electronic structure, is a subject in this dissertation. I describe here a theoretical background in *ab initio* method to introduce the complexity in the electronic structure. The *ab initio* wavefunction theory starts from a Hartree-Fock (HF) method [7] where the many-electron wavefunction is approximated by one single electronic configuration represented by a Slater determinant [8]. The one-electron wavefunction for a molecule is referred to as molecular orbital, which is approximated by a linear combination of basis functions prepared for the composed atoms in a Hartree-Fock-Roothaan (HFR) scheme [9]. As the number of basis functions increases, the HFR solution approaches to the HF solution (Hartree-Fock limit). There remains a difference between the HF solution and a solution of the electronic Schrodinger

equation, which leads to a concept of electron correlation. The electron correlation is categorized to as dynamic correlation and static correlation; the former originates from electronic excitation due to a collision of two electrons, while the latter originates from a resonance of more than two electronic configurations due to a near-degeneracy. When static correlation becomes significant, the HF method breaks down, and a multiconfigurational wavefunction is required to represent the electronic ground state. If there exist near-degenerate electronic states in a low-energy region, a multi-state multireference theory is necessary.

1.5 Relativistic Effects in Atom and Molecule

In addition to the correlation effects, the relativistic effect becomes important especially for heavy elements. As the atomic number increases from the fourth to the fifth period in the periodic table, the significance of the relativistic effect increases more and more, and even if the Schrödinger equation is strictly solved for such a system, the solution does not match the experimental result (Figure 1-1).The fundamental equation for relativistic quantum mechanics is called the Dirac equation [11]. In the 21st century, Nakatsuji developed a new methodology to solve the Schrödinger equation and Dirac equation exactly by his own numerical approaches [12]. There are two categories in relativistic effects, i.e., scalar relativistic effect (mass-velocity, Darwin) and spin-orbit coupling effect. The scalar relativistic effect is concerned with the velocity of inner-shell electrons. In heavy elements, the Coulombic attraction force from the nucleus to electrons becomes large and the expectation value of a velocity of inner-shell electrons becomes close to the

speed of light. Thus, the inner-shell electrons in heavy elements follows the relativistic quantum mechanics theory, the Dirac equation, which affects the behavior of the valence electrons through the orthogonality of the wavefunction. As the results, the relativistic effects influence molecular structures and chemical reactions. The spin-orbit coupling effects are related to the chemical phenomena as spin-forbidden transition and relaxation, intersystem crossing, splitting of energy levels, and so on.

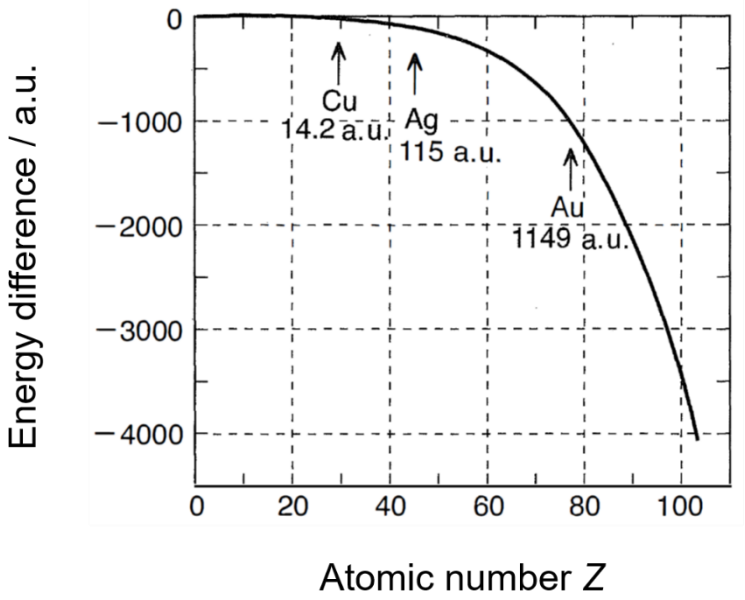

Figure 1-1. The difference between the relativistic and non-relativistic energy of atoms as a function of the atomic number [10].

1.6 Relativistic quantum chemical approach

So far, the relativistic effective core potential (RECP) approach has been used to describe relativistic effects [13] where the core-shell electrons are replaced with an effective potential which affects the valence-shell electrons. The effective potentials are determined by considering the relativistic effects. This approach reduces the number of

electrons, considers the scalar relativistic effect as core-potentials, and can be used in a scheme of non-relativistic theory, so it has been a very useful approach to treat heavy elements, although the core-electrons cannot be treated explicitly. It is noted that the Dirac equation itself leads to the four-component equations which are difficult to solve by numerical approach. In recent developments in relativistic molecular theory, the two-component relativistic method such as the relativistic scheme by eliminating small components (RESC) [14] and Douglas-Kroll-Hess (DKH) methods [15][16] have been proposed and formulated in a practical calculation. To perform the relativistic highly accurate quantum chemistry calculation based on the two-component method, an all-electron basis set considering the dynamic correlation, static correlation, and relativistic effect is required.

1.7 Sapporo basis sets

Noro and Sekiya have developed a family of Sapporo basis sets for the elements in a periodic table systematically [17]. The Sapporo basis sets are designed in a correlation-consistent manner based on a segmented-contraction scheme, and thus, the size is compact and good accuracy is expected. The core-correlation effects are considered in a design of basis sets, and the relativistic effects are taken into account for heavy elements. The Sapporo basis set is available on an official website: segmented GTF basis set factory [18] (the open-page is shown in Figure 1-2), which provides the all-electron basis set for the elements from the first period to the sixth period. Although it has been developed recently, the Sapporo basis set has many advantages and is getting widely used.

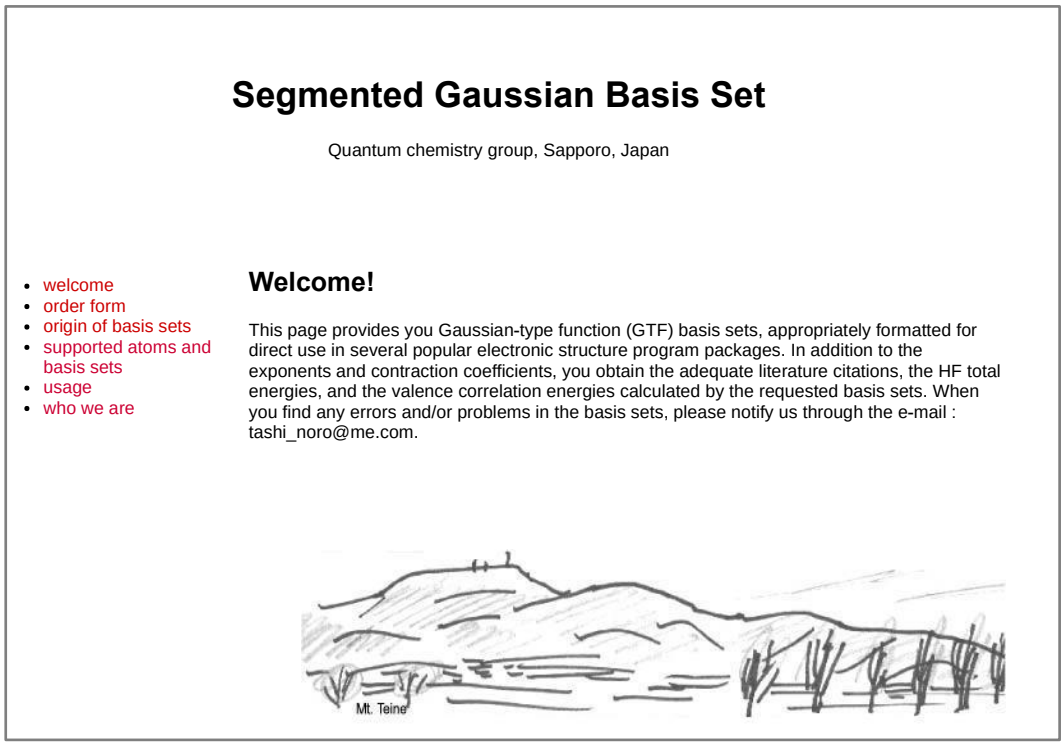

Figure 1-2. The open-page of Sapporo basis set website. The basis sets are available from order form in the menu located in left side of this page.

1.8 Electronic structure in lanthanide atom

The heavy elements having a complex electronic structure include a series of lanthanide (4f-elements) and actinide (5f-elements). Figure 1-3 shows the ground-state configurations of a series of 15 lanthanide atoms. The 6s atomic orbital in the most outer-shell is doubly-occupied, and the inner-shell 4f and 5d atomic orbitals are occupied partially. The lanthanide containing molecules and complexes have a common characteristic of partially-filled atomic orbital (AO)-like 4f orbitals, which often requires some state-average treatments in orbital determining step, and balanced treatments for the static and dynamic correlation effects as well as the scalar and spin-orbit relativistic effects. The magnetic properties of lanthanide single-molecule magnets attract a lot of

attentions due to the possibility of a useful application such as magnetic resonance contrast agents [19]. Soncini and coworkers [20] have very recently proposed an *ab initio* sophisticated approach to the calculations of the electronic structures and magnetic properties of lanthanide complexes, considering both the spin-orbit coupling and ligand-field effects.

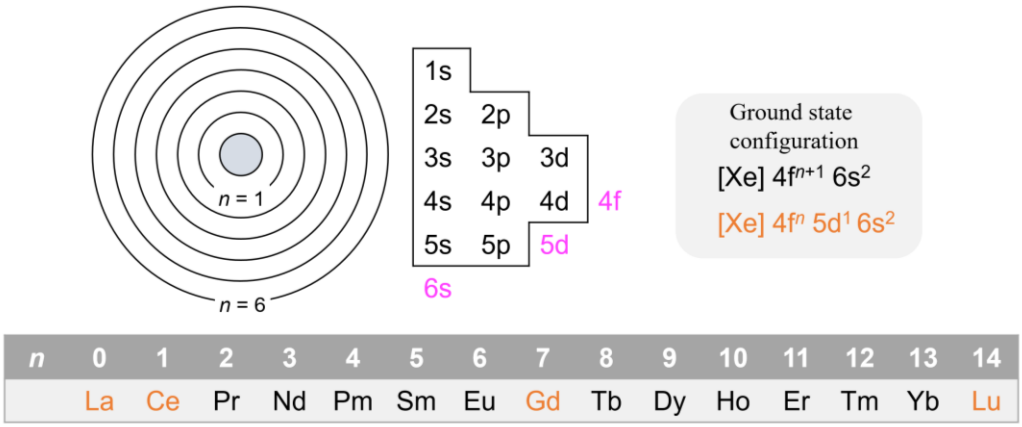

Figure 1-3. A series of lanthanide atoms with the ground-state configurations.

1.9 The final frontier in electronic structure theory

Since the lanthanide atoms and molecules have open-shell configurations due to the inner-shell partially-filled 4f and 5d orbitals, the existence of many closely-lying electronic states make theoretical computations a very hard task. Figure 1-4 shows radial functions of Gd atomic orbitals determined by the ATOMCI program [21]. To consider the correlation effects for 4f electrons, 4s, 4p, and 4d orbitals should be included as correlated orbitals, and of course the basis functions should be prepared to take account of such core correlation effects. In view of these complexity, the highly accurate calculation for atomic

and molecular electronic structure systems containing lanthanide and actinide is the final frontier of electronic structure calculation.

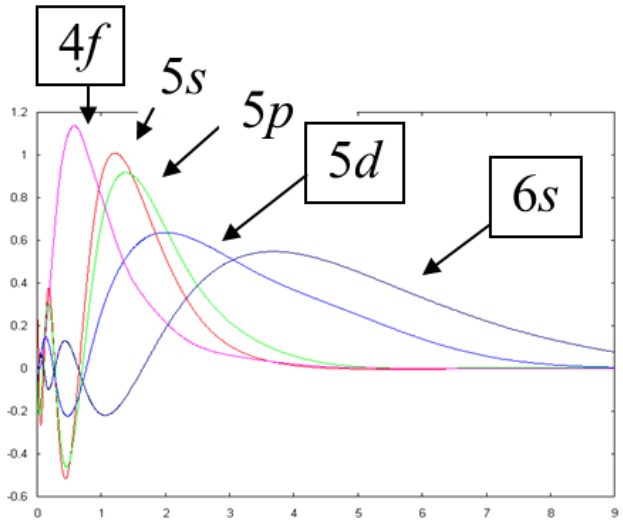

Figure 1-4. Radial wavefunctions of atomic orbitals of Gd atom calculated by ATOMCI.

1.10 The new scheme for complex electronic structure system

The purpose of this thesis is to propose a new computational strategy for accurate calculations of the complex electronic structure systems by considering relativistic and correlations effects in a balanced manner. The new scheme can be summarized as shown below, followed by a schematic picture in Figure 1-5

1. The scalar relativistic effects are taken into account by the third-order Douglas-Kroll approach.
2. The spin-orbit coupling elements are calculated by the state-averaged multi-configuration wavefunctions.

3. The energies of multiple electronic states calculated by the multireference perturbation theory based on the state-averaged multi-configuration wavefunctions are substituted to the diagonal terms in the spin-orbit coupled matrix, for considering both static and dynamic correlation effects.
4. Finally, the energy levels are determined through a diagonalization of the spin-orbit coupled matrix.

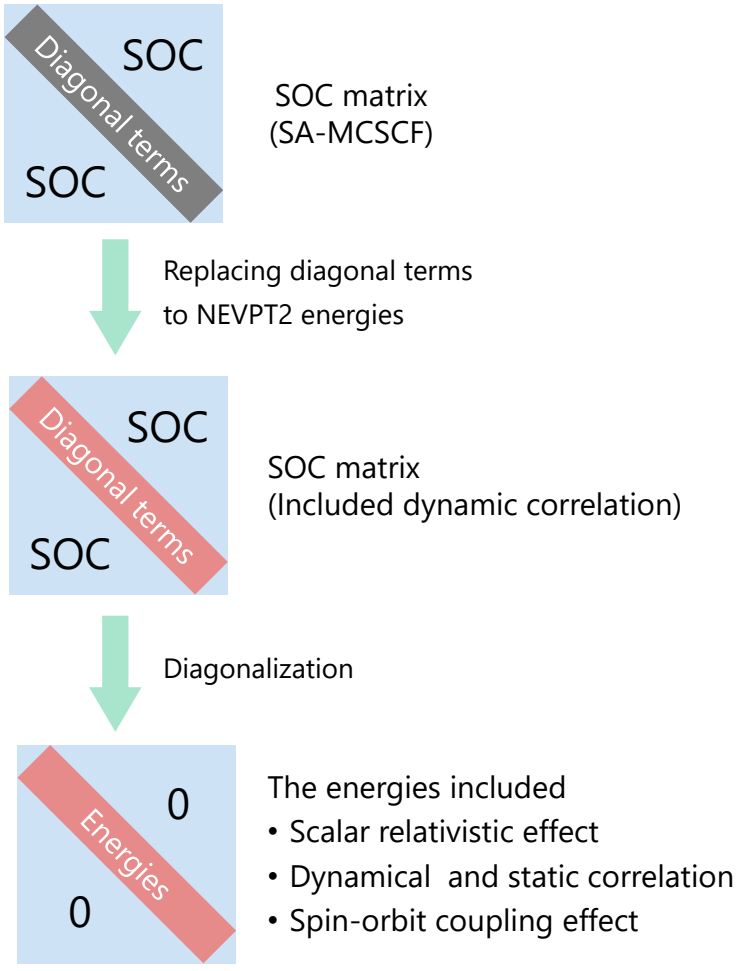

Figure 1-5. The diagram of the new computational scheme.

To realize the above computational strategy, one needs all-electron basis sets which can describe both correlation and relativistic effects appropriately. As already introduced in this section, the Sapporo basis set is just the basis set satisfying all the requirements for this purpose. Thus, I put the Sapporo basis set as a final piece to complete the Jigsaw puzzle for solving quantum chemical problems related to the complex electronic structure system (Figure 1-6).

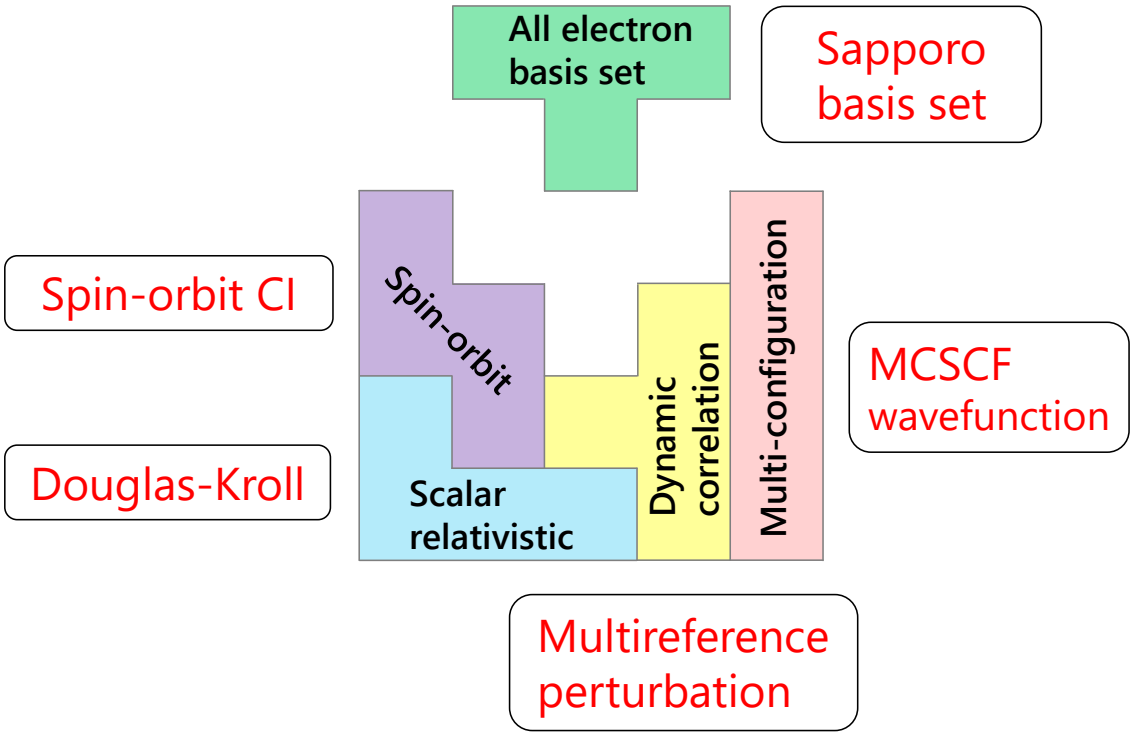

Figure 1-6. The Jigsaw puzzle for the complex electronic structure system.

1.11 Overview of Thesis

This dissertation is organized as follows: Chapter 2 demonstrates that the spin-orbit coupling effects play a key role in determining the electronic ground state of the transition-metal-contained triatomic molecules, PtCN and PtNC. The CCSD(T) high-level computations without spin-orbit coupling predict that the ground states of these species are $^2\Sigma$ state with Pt-d^9 configuration, with the low-lying $^2\Delta$ and $^2\Pi$ states; by including spin-orbit coupling effects, the $^2\Delta_{5/2}$ state becomes the ground state in both PtCN and PtNC, which is in consistent with the spectroscopic experiment. Chapter 3 describes the *ab initio* all-electron computations for the lanthanide atom monovalent cation, Ce^+, taking account of the static and dynamic correlation effects and scalar and spin-orbit relativistic effects, quantitatively. Following the computational scheme to evaluate the spin-orbit coupled states shown in Figure 1-5, the low-lying energy levels of Ce^+ with the electronic configurations, $[Xe]4f^15d^16s^1$ and $[Xe]4f^15d^2$, are calculated by the SA-RASSCF(CASSCF)/NEVPT2+SOCI method, and the accuracy of the all-electron basis sets taking the relativistic effects into account is evaluated. Chapter 4 presents the ground state, low-lying excited state, and spectroscopic constants of CeF under the same calculation scheme for Ce^+. It is shown that the ground-state configuration and the excited-state configuration change to $[Xe]4f^15d^2$ and $[Xe]4f^15d^16s^1$ respectively. In Chapter 5, the ground and excited states of CeH are calculated in the same way to CeF in Chapter 4. CeH has both covalent-bond and ionic-bond characters, which is different from an ionic-bond system, CeF. The ground state for CeH is identified to be quartet, with very-low-lying doublet states. Finally, concluding remarks are given in Chapter 6.

1.12 References

[1] E. Schrödinger, Annalen der Physik, **79**, 361 (1926); **79**, 489 (1926); **80**, 434 (1926); **81**, 109 (1926).

[2] P. Hohenberg and W. Kohn, Phys. Rev., **136**, B864 (1964).

[3] D. G. Fedorov and K. Kitaura (ed.), "The Fragment Molecular Orbital Method: Practical Applications to Large Molecular Systems," CRC Press, Boca Raton, Florida, (2009).

[4] M. Kobayashi, Y. Imamura, and H. Nakai, J. Chem. Phys., **127**, 074103 (2007).

[5] H. M. Senn and W. Thiel, Angew. Chem. Int. Ed., **48**, 1198 (2009).

[6] L. W. Chung, W. M. C. Sameera, R. Ramozzi, A. J. Page, M. Hatanaka, G. P. Petrova, T. V. Harris, X. Li, Z. Ke, F. Liu, H.-B. Li, L. Ding, and K. Morokuma, Chem. Rev., **115**, 5678 (2015).

[7] V. Fock, Z. Phys., **61**, 126 (1930).

[8] J. C. Slater, Phys. Rev., **34**, 1293 (1929).

[9] C. C. J. Roothaan, Rev. Mod. Phys., **23**, 69 (1951).

[10] S. Nagase and K. Hirao, R. Okazaki (Eds.), Gendai kagaku heno nyumon 17 (Introduction to modern chemistry 17), Iwanami, (2002), ISBN: 9784000110471, p.76.

[11] P. A. M. Dirac, Proc. Royal Soc. A, **117**, 610 (1928).

[12] H. Nakatsuji, J. Chem. Phys., **113**, 2949 (2000).

[13] M. Dolg (Ed.), Computational Methods in Lanthanide and Actinide Chemistry, John Wiley & Sons, (2015).

[14] T. Nakajima and K. Hirao, Chem. Phys. Lett., **302**, 383 (1999).

[15] B. A. Hess, Phys. Rev. A, **33**, 3742 (1986).

[16] T. Nakajima, K. Hirao, J. Chem. Phys., **113**, 7786 (2000).

[17] M. Sekiya, T. Noro, T. Koga, and T. Shimazaki, Theor. Chem. Acc., **131**, 1247 (2012); T. Noro, M. Sekiya, and T. Koga, Theor. Chem. Acc., **131**, 1124 (2012); **132**, 1363 (2013).

[18] T. Noro, Segmented GTF basis set factory. http://sapporo.center.ims.ac.jp/sapporo/ (accessed December 8, 2017).

[19] M. Bottrill, L. Kwok, and N. J. Long, Chem. Soc. Rev., **35**, 557 (2006).

[20] S. Calvello, M. Piccardo, S. V. Rao, and A. Soncini, J. Comput. Chem., (2017), DOI: 10.1002/jcc.25113.

[21] ATOMCI: F. Sasaki, M. Sekiya, T. Noro, K. Ohtsuki, and Y. Osanai, METECC-94. STEF, Cagliari (1993).

2. Spin-Orbit Coupling Effects on the Low-Lying Electronic States of PtCN/PtNC and PdCN/PdNC

2.1 Introduction

The platinum atom is a transition metal element in the sixth period of the periodic table where relativistic effects play a significant role. Due to recent progresses of a molecular theory, it has become feasible to evaluate the spectroscopic constants of the transition metal compounds containing Pt atoms quantitatively by applying the state-of-the-art *ab initio* molecular orbital theory that can treat both relativistic effects and electron correlation effects appropriately. Nowadays theoretical calculations play an important role in understanding and predicting the spectroscopic constants of the molecules in cooperation with experiments.

Here, I introduce the case of PtCN, as an example. The bonding nature in PtCN is an ionic bond between Pt^+ and CN^-; the ground *LS* term and electronic configuration of Pt^+ is ^2D with the $(5d)^9$, so that the electronic terms of the ground states of PtCN are $^2\Sigma$, $^2\Pi$, and $^2\Delta$. By theoretical calculations, the electronic ground state of PtCN was predicted to be $^2\Sigma$ [1], but recently it was reported that the angular momentum of the electronic ground state about the Pt-C-N bond axis was $\Omega = 5/2$, originating from $^2\Delta$, by the measurement of a millimeter wave spectrum and the submillimeter wave spectrum [2], where Ω denotes a quantum number for the total electronic angular momentum around the molecular axis as shown in Figure 2-1. Ono et al. performed theoretical calculations for PtCN and PtNC and reported preliminary results that their ground states were

predicted to be $^2\Delta_{5/2}$ by considering spin-orbit coupling effects at the meeting [3]. The other group also reported similar results for PtCN and PdCN, by theoretical calculations including spin-orbit coupling effects [4].

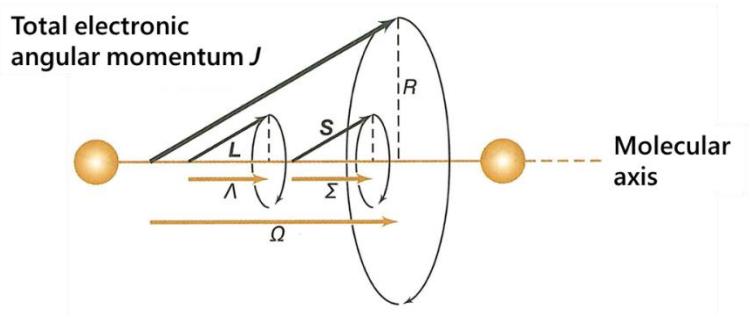

Figure 2-1. The schematic diagram of quantum number Ω [5].

In this chapter, I reported a summary of quantum chemical calculations for the low-lying electronic states of PtCN and PtNC, to identify the electronic ground state and to determine the equilibrium structures and vibrational frequencies, by the highly-accurate electronic structure theory, taking into account the scalar and spin-orbit relativistic effects and electron correlation effects [6]. It is noted that there is no report of the experimental observation for PtNC. I also performed a set of the same calculations for PdCN and PdNC for comparisons [6]. As to PdCN, Okabayashi and coworkers performed the similar experiments to determine the ground state term, equilibrium geometries, and the Pd-C vibrational frequency [7].

2.2 Computational Details

The electronic ground state of Pt is known to be ^{3}D with the $(5d)^9(6s)^1$ configuration, while the ground state of Pd is ^{1}S with the $(4d)^{10}$ configuration. The ground state of CN

is $^2\Sigma$ with an unpaired electron in 5σ orbital. Through a binding of Pt (6s) and CN (5σ) in a linear form (PtCN or PtNC), the ground state of Pt (^{3}D) splits to $^2\Sigma$, $^2\Pi$, and $^2\Delta$ states under the $C_{\infty v}$ point group. Both PdCN and PdNC also have $^2\Sigma$, $^2\Pi$, and $^2\Delta$ states in the low-lying region in a linear form. I employed a sub-group of $C_{\infty v}$, *i.e.*, C_{2v}, in the present calculations where 1^2A_1, 1^2B_1 and 1^2A_2 are regarded as $^2\Sigma$, $^2\Pi$, and $^2\Delta$ states, respectively. The energy was calculated for these three electronic states by the spin-restricted open-shell coupled cluster singles and doubles with a perturbational estimate of triple-excitations (RCCSD(T)). The relativistic effects were taken into account by the third-order Douglas-Kroll relativistic one-electron integrals [8], with relativistic basis sets, Sapporo-DKH3-QZP [9],[10].

The spin-orbit coupling elements were also calculated for $^2\Sigma$, $^2\Pi$, and $^2\Delta$ states of PtCN, PtNC, PdCN, and PdNC, as well as the ground state of Pt atom (^{3}D), using the Breit-Pauli Hamiltonian scheme [11], by the state-averaged complete-active-space multi-configurational self-consistent field (SA-CASSCF) method, and the energy levels of spin-orbit-coupled states were calculated through a diagonalization of the spin-orbit coupling matrix where the diagonal terms are replaced with the RCCSD(T) energy for the respective electronic states. Under the assumption of linear geometry for PtCN, PtNC, PdCN, and PdNC, two-dimensional potential energy surfaces were determined for spin-orbit uncoupled ($^2\Sigma$, $^2\Pi$, and $^2\Delta$) and spin-orbit-coupled states of both compounds to determine the equilibrium bond lengths and vibrational frequencies of stretching modes. All quantum chemical calculations were carried out with the MOLPRO2010 program package [12].

2.3 Results and Discussion

Table 2-1 shows the equilibrium bond lengths, harmonic frequencies, and relative energies of $^2\Sigma$, $^2\Pi$, and $^2\Delta$ states of PtCN, PtNC, PdCN, and PdNC by RCCSD(T) calculations, without spin-orbit coupling effects. In all the compounds $^2\Sigma$ is the ground state, with $^2\Delta$ the second lowest for PtCN, PtNC, and PdCN, while $^2\Pi$ the second lowest for PdNC. The energy of the $^2\Delta$ state relative to the $^2\Sigma$ state is relatively small, i.e., 4.3 and 4.2 kcal/mol, for PtCN and PtNC, respectively, while the energy difference for the ground and first-excited state for PdCN and PdNC is relatively large, i.e., 20.3 and 14.7 kcal/mol, respectively. The $^2\Sigma$ state of PtNC is 26.4 kcal/mol higher than that of PtCN, which is consistent with no experimental observation of PtNC. Similarly, the $^2\Sigma$ state of PdNC is 20.3 kcal/mol higher than that of PdCN. For PtCN, the equilibrium distance of Pt-C was calculated to be 1.8772 Å and 1.9028 Å in the $^2\Sigma$ and $^2\Delta$ states, respectively, and the latter bond length is much closer to the experimental values, 1.90114 Å (r_0) and 1.89872 Å ($r^{(2)}_m$ that is approximation to r_e), measured for the ground state of PtCN with $\Omega = 5/2$ [2]. For PdCN, the equilibrium distance of Pd-C was calculated to be 1.9132 Å in the $^2\Sigma$ state that is very close to the experimental value, 1.9280 Å (r_0) [7]. The binding energy for Pt-CN ($^2\Sigma$) was calculated to be 103.9 kcal/mol as the stabilization energy from the dissociation limit of Pt (^{3}D) and CN ($^2\Sigma$), at the RCCSD(T) level. The corresponding binding energy for Pd-CN ($^2\Sigma$) was calculated to be 71.8 kcal/mol.

Table 2-1. The equilibrium bond lengths (in Å), harmonic frequencies (in cm^{-1}), and relative energies of $^2\Sigma$, $^2\Delta$, and $^2\Pi$ states of PtCN, PtNC, PdCN and PdNC without spin-orbit coupling corrections (in kcal/mol).

PtCN	*r*(Pt-C)	*r*(C-N)	ν(PtC)	ν(CN)	Rel.En	
$^2\Sigma$	1.8772	1.1679	526	2176	0.0	
$^2\Delta$	1.9028	1.1661	516	2204	4.3	
$^2\Pi$	1.8874	1.1739	466	2048	13.0	
Exp.						
r_0: $^2\Delta_{5/2}$	1.90114	1.16073	510			[2]
$r^{(2)}_m$: $^2\Pi_{5/2}$	1.89872	1.16241				
PtNC	*r*(Pt-N)	*r*(N-C)	ν(PtN)	ν(NC)	Rel.En.	
$^2\Sigma$	1.8861	1.1798	509	2090	26.4	
$^2\Delta$	1.9099	1.1795	497	2101	30.6	
$^2\Pi$	1.8795	1.1871	484	2011	33.3	
PdCN	*r*(Pd-C)	*r*(C-N)	ν(PdC)	ν(CN)	Rel.En.	
$^2\Sigma$	1.9132	1.1669	443	2167	0.0	
$^2\Delta$	2.0009	1.1657	436	2189	20.3	
$^2\Pi$	2.0169	1.1689	417	2135	21.5	
Exp.						
r_0: $^2\Sigma_{1/2}$	1.9280	1.1742	439			[7]
PdNC	*r*(Pd-N)	*r*(N-C)	N(PdN)	ν(NC)	Rel.En.	
$^2\Sigma$	1.9378	1.1780	458	2104	20.3	
$^2\Pi$	1.9963	1.1823	431	2062	35.0	
$^2\Delta$	2.0106	1.1780	439	2111	38.5	

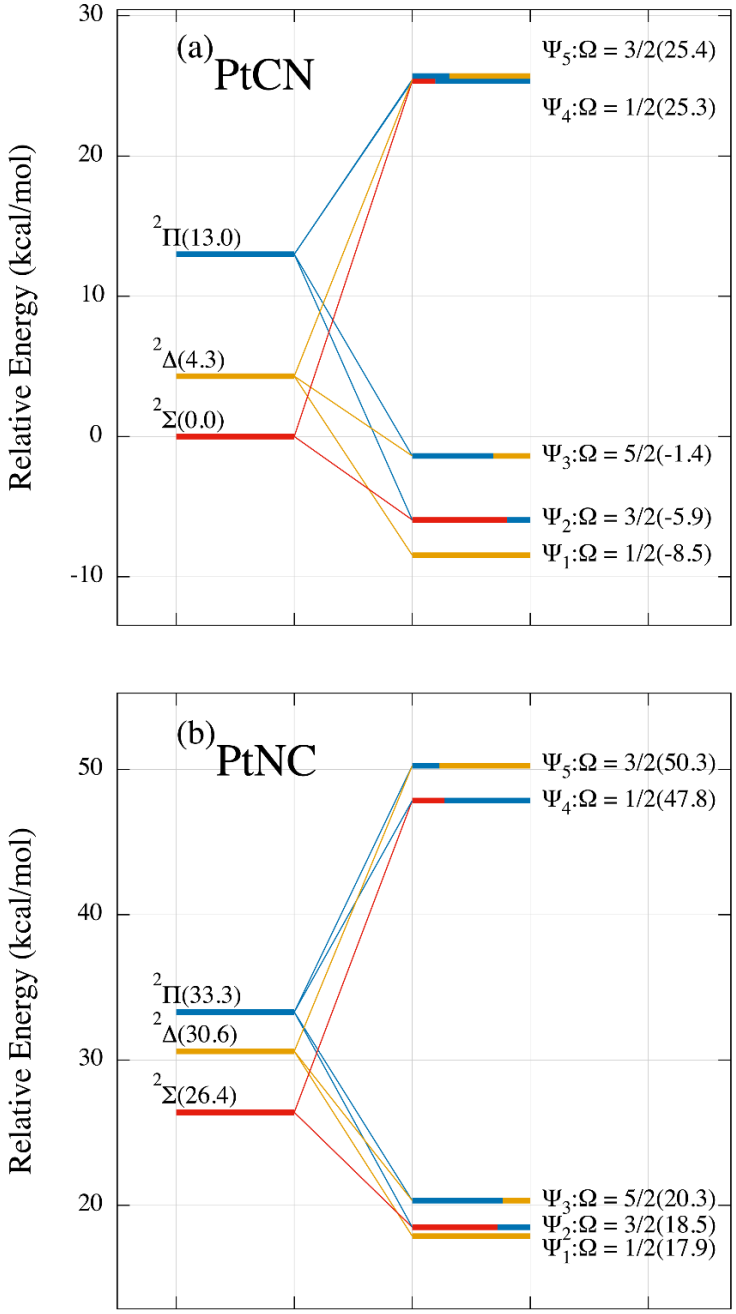

Figure 2-2. The correlation diagram of spin-orbit uncoupled and coupled states calculated at the equilibrium geometry of the ground state $\Psi_1(\Omega = 5/2)$ for (a) PtCN and (b) PtNC.

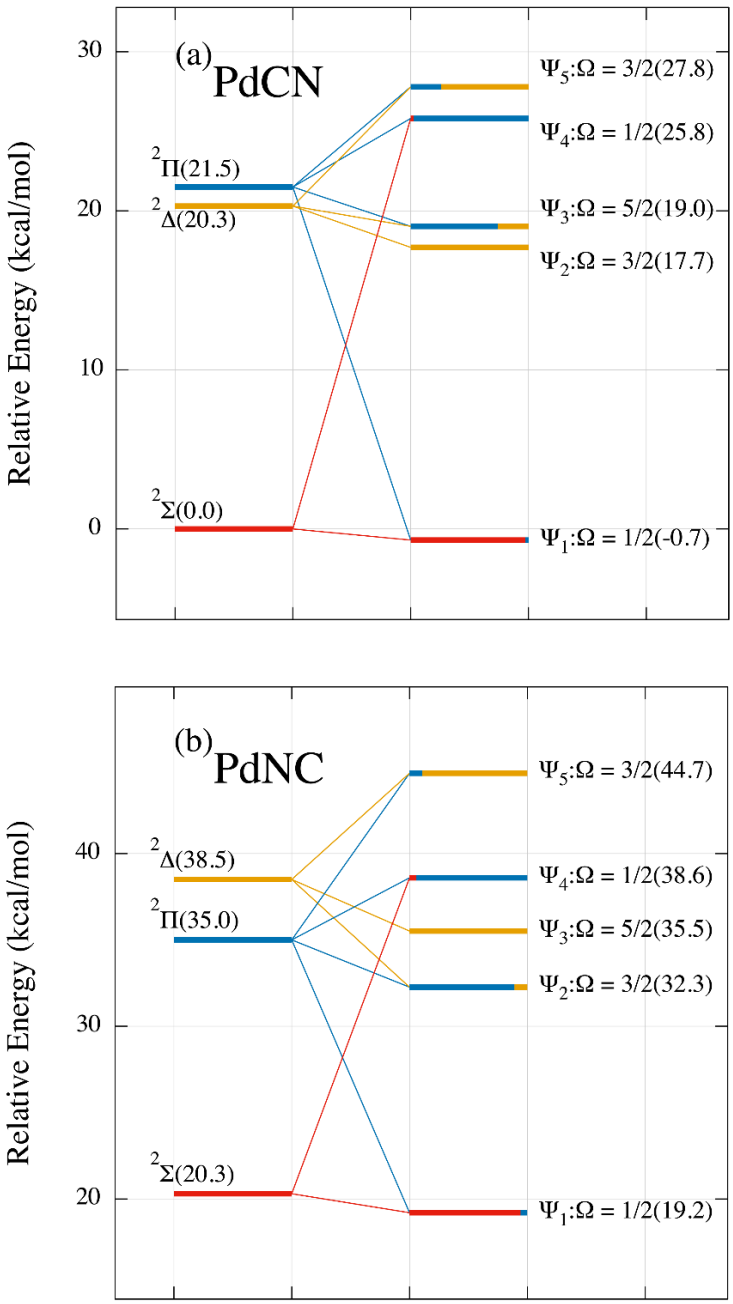

Figure 2-3. The correlation diagram of spin-orbit uncoupled and coupled states calculated at the equilibrium geometry of the ground state $\Psi_1(\Omega = 1/2)$ for (a) PdCN and (b) PdNC.

Figure 2-2 shows the correlation diagram of spin-orbit uncoupled states ($^2\Sigma$, $^2\Pi$, $^2\Delta$) and coupled states (Ω =1/2, 1/2, 3/2, 3/2, 5/2) calculated at the equilibrium geometry of the ground state Ψ_1 for PtCN and PtNC. Figure 2-3 shows the corresponding diagram for PdCN and PdNC. In PtCN and PtNC, the character of the ground state changes from $^2\Sigma$ to $^2\Delta$ by the spin-orbit coupling effect, and the ground state is shown to be $\Psi_1(\Omega = 5/2)$, which is in agreement with the experimental observation. The first excited state is $\Psi_2(\Omega = 1/2)$ which consists of $^2\Sigma$ and $^2\Pi$, while the second excited state is $\Psi_3(\Omega = 3/2)$ which consists of $^2\Pi$ and $^2\Delta$. The energies of the first excited state relative to the ground state are calculated to be 2.5 and 0.6 kcal/mol for PtCN and PtNC, respectively. In PdCN and PdNC, the ground state remains as $^2\Sigma$ character, with a slight mixing of $^2\Pi_{1/2}$, even after considering the spin-orbit coupling effects. It is noted that, in PdCN and PdNC cases, there is a relatively large energy difference between the ground and first excited states in the spin-orbit uncoupled states.

Table 2-2 shows the mixing weights for the spin-orbit coupled states at the equilibrium geometry of the ground state Ψ_1, as well as the equilibrium bond distances for the respective electronic states, for PtCN, PtNC, PdCN, and PdNC. For Pt-compounds, the ground state, $\Psi_1(\Omega = 5/2)$, is contributed from only the $^2\Delta$ state, and thus, the bond distances are the same for $^2\Delta$ (Table 1) and $\Psi_1(\Omega = 5/2)$ states (Table 2-2), which are in good agreement with the experimental values. On the other hand, as to other electronic states (Ω = 1/2, 3/2), two electronic states mix in with each other, and the calculated bond lengths are shown to be a weighted average of those of spin-orbit uncoupled states. The binding energy for Pt-CN ($\Psi_1(\Omega = 5/2)$) was calculated to be 109.3 kcal/mol as the

stabilization energy from the dissociation limit of Pt ($^3D_3$) and CN ($^2\Sigma$), which is slightly larger than the spin-orbit-uncoupled result, 103.9 kcal/mol. The corresponding binding energy for Pd-CN ($\Psi_1(\Omega = 1/2)$) was calculated to be 73.1 kcal/mol, which is also similar to the spin-orbit-uncoupled value, 71.8 kcal/mol.

Table 2-2. The mixing weights for spin-orbit coupled states of PtCN, PtNC, PdCN and PdNC, with the equilibrium bond distances (in Å).

PtCN	Mixing Weight	*r*(Pt-C)	*r*(C-N)
$\Psi_1(\Omega=5/2)$	$^2\Sigma_{5/2}(100\%)$	1.9026	1.1659
$\Psi_2(\Omega=1/2)$	$^2\Sigma_{1/2}(80.6\%) + {}^2\Pi_{1/2}(19.4\%)$	1.8919	1.1684
$\Psi_3(\Omega=3/2)$	$^2\Pi_{3/2}(68.8\%) + {}^2\Delta_{3/2}(31.2\%)$	1.8999	1.1701
$\Psi_4(\Omega=1/2)$	$^2\Sigma_{1/2}(19.4\%) + {}^2\Pi_{1/2}(80.6\%)$	1.8691	1.1734
$\Psi_5(\Omega=3/2)$	$^2\Pi_{3/2}(31.2\%) + {}^2\Delta_{3/2}(68.8\%)$	1.8924	1.1696
PtNC	Mixing Weight	*r*(Pt-N)	*r*(N-C)
$\Psi_1(\Omega=5/2)$	$^2\Delta_{5/2}(100\%)$	1.9095	1.1793
$\Psi_2(\Omega=1/2)$	$^2\Sigma_{1/2}(72.6\%) + {}^2\Pi_{1/2}(27.4\%)$	1.8967	1.1813
$\Psi_3(\Omega=3/2)$	$^2\Pi_{3/2}(77.2\%) + {}^2\Delta_{3/2}(22.8\%)$	1.8906	1.1845
$\Psi_4(\Omega=1/2)$	$^2\Sigma_{1/2}(27.4\%) + {}^2\Pi_{1/2}(72.6\%)$	1.8626	1.1867
$\Psi_5(\Omega=3/2)$	$^2\Pi_{3/2}(23.0\%) + {}^2\Delta_{3/2}(77.0\%)$	1.9041	1.1811
PdCN	Mixing Weight	*r*(Pd-C)	*r*(C−N)
$\Psi_1(\Omega=1/2)$	$^2\Sigma_{1/2}(97.4\%) + {}^2\Pi_{1/2}(2.6\%)$	1.9175	1.1667
$\Psi_2(\Omega=5/2)$	$^2\Delta_{5/2}(100\%)$	2.0041	1.1654
$\Psi_3(\Omega=3/2)$	$^2\Pi_{3/2}(75.8\%) + {}^2\Delta_{3/2}(24.2\%)$	2.0213	1.1677
$\Psi_4(\Omega=1/2)$	$^2\Sigma_{1/2}(3.7\%) + {}^2\Pi_{1/2}(96.3\%)$	2.0177	1.1685
$\Psi_5(\Omega=3/2)$	$^2\Pi_{3/2}(24.5\%) + {}^2\Delta_{3/2}(75.5\%)$	2.0090	1.1662
PdNC	Mixing Weight	*r*(Pd-N)	*r*(N-C)
$\Psi_1(\Omega=1/2)$	$^2\Sigma_{1/2}(94.3\%) + {}^2\Pi_{1/2}(5.7\%)$	1.9424	1.1780
$\Psi_2(\Omega=3/2)$	$^2\Pi_{3/2}(88.5\%) + {}^2\Delta_{3/2}(11.5\%)$	1.9989	1.1816
$\Psi_3(\Omega=5/2)$	$^2\Delta_{5/2}(100\%)$	2.0123	1.1778
$\Psi_4(\Omega=1/2)$	$^2\Sigma_{1/2}(6.5\%) + {}^2\Pi_{1/2}(93.5\%)$	1.9908	1.1820
$\Psi_5(\Omega=3/2)$	$^2\Pi_{3/2}(11.6\%) + {}^2\Delta_{3/2}(88.4\%)$	2.0105	1.1783

2.4 Conclusion

The spin-orbit coupling effects play a key role to determine the ground state of the triatomic molecules PtCN, PtNC, PdCN, and PdNC. These molecular systems have a doublet spin-multiplicity, and one unpaired-electron occupies one of five d orbitals in Pt or Pd. So, there are five nearly-degenerate electronic states in the ground-state energy region. The highly-accurate CCSD(T) energies and SA-CASSCF spin-orbit coupling terms are used to calculate the energy levels of the spin-orbit coupled states. Without a spin-orbit coupling, the ground state of PtCN is shown to be $^2\Sigma$, while with a spin-orbit coupling, the ground state is shown to be $^2\Delta_{5/2,}$ which is consistent with the experiment.

2.5 References

[1] B. Chatterjee, F. A. Akin, C. C. Jarrold, and K. Raghavachari, J. Phys. Chem. A, **109**, 6880 (2005).

[2] E. Y. Okabayashi, T. Okabayashi, T. Furuya, and M. Tanimoto, Chem. Phys. Lett., **492**, 25 (2010).

[3] Y. Ono, T. Noro, and T. Taketsugu, the Annual Meeting of Japan Society for Molecular Science (2011), Sapporo, Sep. 20-23, 2011, Abstr., No. 2P130.

[4] J. Moon and J. Kim, PHYS 565, Pacifichem2015.

[5] D. W. Ball, translated by K. Tanaka and T. Atake, Physical chemistry (second edition, second volume), Kagaku-Dojin, (2015), ISBN: 9784759817904, p.636.

[6] Y. Ono, Y. Kondo, M. Kobayashi, and T. Taketsugu, Chem. Lett., **45**, 478 (2016).

[7] Y. Kise, E. Y. Okabayashi, T. Okabayashi, the 9th Symposium on Molecular Spectroscopy, Toyama Univ., May 15-16, 2009; private communication.

[8] M. Reiher and A. Wolf, J. Chem. Phys. **121**, 2037 (2004); M. Reiher and A. Wolf, J. Chem. Phys. **121**, 10945 (2004); A. Wolf, M. Reiher, and B. A. Hess, J. Chem. Phys. **117**, 9215 (2002).

[9] T. Noro, M. Sekiya, T. Koga, Theoret. Chem. Acc. **131**, 1124 (2012).

[10] T. Noro, M. Sekiya, T. Koga, Theoret. Chem. Acc. **132**, 1363 (2013).

[11] A. Berning, M. Schweizer, H.-J. Werner, P. J. Knowles, and P. Palmieri, Mol. Phys., **98**, 1823-1833 (2000)

[12] MOLPRO, version 2010.1, a package of *ab initio* programs, H.-J. Werner, P. J. Knowles, G. Knizia, F. R. Manby, M. Schütz, P. Celani, T. Korona, R. Lindh, A. Mitrushenkov, G.

Rauhut, K. R. Shamasundar, T. B. Adler, R. D. Amos, A. Bernhardsson, A. Berning, D. L. Cooper, M. J. O. Deegan, A. J. Dobbyn, F. Eckert, E. Goll, C. Hampel, A. Hesselmann, G. Hetzer, T. Hrenar, G. Jansen, C. Köppl, Y. Liu, A. W. Lloyd, R. A. Mata, A. J. May, S. J. McNicholas, W. Meyer, M. E. Mura, A. Nicklass, D. P. O'Neill, P. Palmieri, K. Pflüger, R. Pitzer, M. Reiher, T. Shiozaki, H. Stoll, A. J. Stone, R. Tarroni, T. Thorsteinsson, M. Wang, and A. Wolf.

3. All-Electron Relativistic Spin-Orbit Computations on the Low-Lying Excited States of Ce^+

3.1 Introduction

For the lanthanide compounds, the relativistic effective core potential (RECP) approach [1] has been widely used for a long time. Yabushita and coworkers [2] employed three different RECPs to investigate the low energy spin-orbit multiplet terms of trivalent lanthanide cations, Ln^{3+}, including the spin-orbit coupling effect explicitly by the full-variational spin-orbit configuration interaction (SOCI) method, and found that semi-core correlations in the 4d, 5s, and 5p shells are significant to reproduce the higher *LS* terms. Taketsugu and coworkers employed a state-averaged complete active space multiconfigurational self-consistent field (SA-CASSCF) method with the RECP to discuss the electronic and geometric structures of a series of the lanthanide trihalides, LnX_3 (Ln = La-Lu; X = F, Cl), including spin-orbit coupling effect explicitly [3].

Recently, the sophisticated two-component relativistic methods such as the relativistic scheme by eliminating small components (RESC) [4] and Douglas-Kroll-Hess (DKH) methods [5][6] have been proposed. Along this two-component relativistic approach, several all-electron relativistic basis sets have been developed for lanthanides, such as Sapporo-DKH3-*X*ZP-2012 [7], ANO-RCC [8], and cc-pwCV*X*Z [9] (*X* = D, T, and Q). Noro and Sekiya have developed a family of Sapporo basis sets for the elements in a periodic table systematically [7],[10]-[12]. The Sapporo basis sets are designed in a correlation-consistent manner based on a segmented-contraction scheme, and thus, the

size is compact and good accuracy is expected.

In this chapter, I report all-electron *ab initio* multiconfigurational/mutireference study on the ground and low-lying excited states of Ce^+, based on a two-component relativistic scheme.

3.2 Computational Details

The early lanthanide atom, Ce, has the ground-state configuration of $[Xe]4f^15d^16s^2$, while the Ce^+ ion has the ground-state configuration of $[Xe]4f^15d^2$ [13]. I calculated the excitation energies of the nearly-degenerate low-lying quartet states of Ce^+ that originate from the ground-state configuration, $[Xe]4f^15d^2$, and from the excited-state configuration, $[Xe]4f^15d^16s^1$, with RECP and all-electron computations. In the RECP calculations, Dolg's RECP [14] combined with def2-QZVPP (11s8p6d5f) basis set [15] was employed, while in the all-electron computations, ANO-RCC (12s11p8d7f4g2h) [8], Sapporo-DKH3-QZP-2012 (13s11p9d7f4g3h1i) [7], and cc-pwCVQZ (13s12p10d9f7g4h1i) [9] relativistic basis sets were employed with the third-order Douglas-Kroll one-electron integrals [16] for the scalar relativistic effects. The numbers of basis functions are 100, 192, 222, and 282 for def2-QZVPP, ANO-RCC, Sapporo-DKH3-QZP-2012, and cc-pwCVQZ, respectively; def2-QZVPP and ANO-RCC were designed so that the correlated orbitals are 4f, 5spd (5s, 5p, 5d), and 6s whereas Sapporo-DKH3-QZP-2012 and cc-pwCVQZ were designed so that the correlated orbitals are 4spdf (4s, 4p, 4d, 4f), 5spd, and 6s. All the electronic structure calculations were carried out with the MOLPRO2012 program package [17],[18].

For Ce^+, the state-averaged restricted active space self-consistent field (SA-RASSCF) method [19] was employed for 70 quartet states of the $[Xe]4f^15d^2$ configuration and 35 quartet states of the $[Xe]4f^15d^16s^1$ configuration separately, with the active space of 3 electrons in 13 orbitals. The state-average scheme is used to get a set of orbitals for describing the nearly-degenerate multi-states equally, and thus, the obtained orbitals are not optimal for the respective states. It is noted that the state-average scheme can reproduce the degeneracy of the electronic states correctly. Succeedingly, the *n*-electron valence state second-order multireference perturbation theory (NEVPT2) with a strongly-contracted scheme [20]-[22] was employed based on the SA-RASSCF zeroth-order wavefunction to estimate the dynamic correlation energy for the respective SA-RASSCF states. In the NEVPT2 calculations, 4f, 5spd, and 6s orbitals were included to estimate the dynamic correlation energy for def2-QZVPP and ANO-RCC basis sets, while 4spdf, 5spd, and 6s orbitals were included as correlated orbitals for Sapporo-DKH3-QZP-2012 and cc-pwCVQZ basis sets. The additional calculation with Sapporo-DKH3-QZP-2012 involving only 4f, 5spd, and 6s as correlated orbitals was also performed to show the core-correlation effects explicitly. In the Breit–Pauli Hamiltonian scheme [23], the spin-orbit coupling matrix was generated for 280 electronic states (from the ground-state configuration with quartet) and for 140 electronic states (from the excited-state configuration with quartet) based on the SA-RASSCF wavefunction. Then, the SA-RASSCF energies for the respective electronic states in the diagonal terms were replaced with the corresponding NEVPT2 energies, followed by a diagonalization of the resultant spin-orbit coupling matrix to evaluate the energy levels of the spin-orbit-coupled states

(referred to as spin-orbit configuration interaction: SOCI). The present SA-RASSCF/NEVPT2+SOCI computations were also performed for 420 states including both $[Xe]4f^{1}5d^{2}$ and $[Xe]4f^{1}5d^{1}6s^{1}$ configurations of quartet to discuss the mixing of these two ensembles of different electronic configurations.

The experimental data [13] indicate that the ground state of Ce^{+} is quartet ($^{4}H_{7/2}$) with a considerable mixing of the doublet lowest state ($^{2}G_{7/2}$). To examine a mixing with the doublet states, I carried out additional calculations for selected low-lying quartet and doublet states by applying the SA-CASSCF/NEVPT2+SOCI approach. It is noted that SOCI calculations including doublet and quartet states using the MOLPRO program [17][18] require the SA-CASSCF wavefunction (SA-RASSCF does not work). The SA-CASSCF active space in this calculation is defined as 3 electrons in 12 orbitals (seven 4f and five 5d orbitals).

3.3 Results and Discussion

I first discuss the electron correlation effects on the relative energies of the low-lying quartet states of Ce^{+}. The atomic terms, ^{2S+1}L (L and S denote quantum numbers of the resultant orbital angular momentum and the resultant spin angular momentum, respectively), are ^{4}S, ^{4}P, $^{4}D\times2$, $^{4}F\times2$, $^{4}G\times2$, ^{4}H, and ^{4}I for the ground-state configuration $[Xe]4f^{1}5d^{2}$ and ^{4}P, ^{4}D, ^{4}F, ^{4}G, and ^{4}H for the excited-state configuration $[Xe]4f^{1}5d^{1}6s^{1}$. Due to the spin-orbit coupling effect, these electronic states mix in with each other, and the spin-orbit coupled states, $^{2S+1}L_{J}$, are classified according to the total angular momentum quantum number J ($|L - S| \leq J \leq L + S$). Here, in order to discuss the electron

correlation effects on the relative energies of the low-lying electronic states, the excitation energies for the spin-orbit uncoupled states, $E(^{2S+1}L)$, are compared with each other. As the reference energies, the experimental excitation energies for the spin-orbit uncoupled states (J-averaged value) were estimated from the experimental energy levels of the spin-orbit coupled states, $E_{\mathrm{exp}}(^{2S+1}L_J)$, by the following equation:

$$E\left(^{2S+1}L\right)=\frac{\sum_{J=|L-S|}^{L+S}(2J+1)E_{\mathrm{exp}}\left(^{2S+1}L_J\right)}{(2S+1)(2L+1)} \quad \textbf{(1)}$$

This is of course an approximation formula in the sense that it does not take account of the contributions from the other ^{2S+1}L states in $E_{\mathrm{exp}}(^{2S+1}L_J)$, and actually in the experimental data book [13], a J-averaged value is missing for some electronic terms.

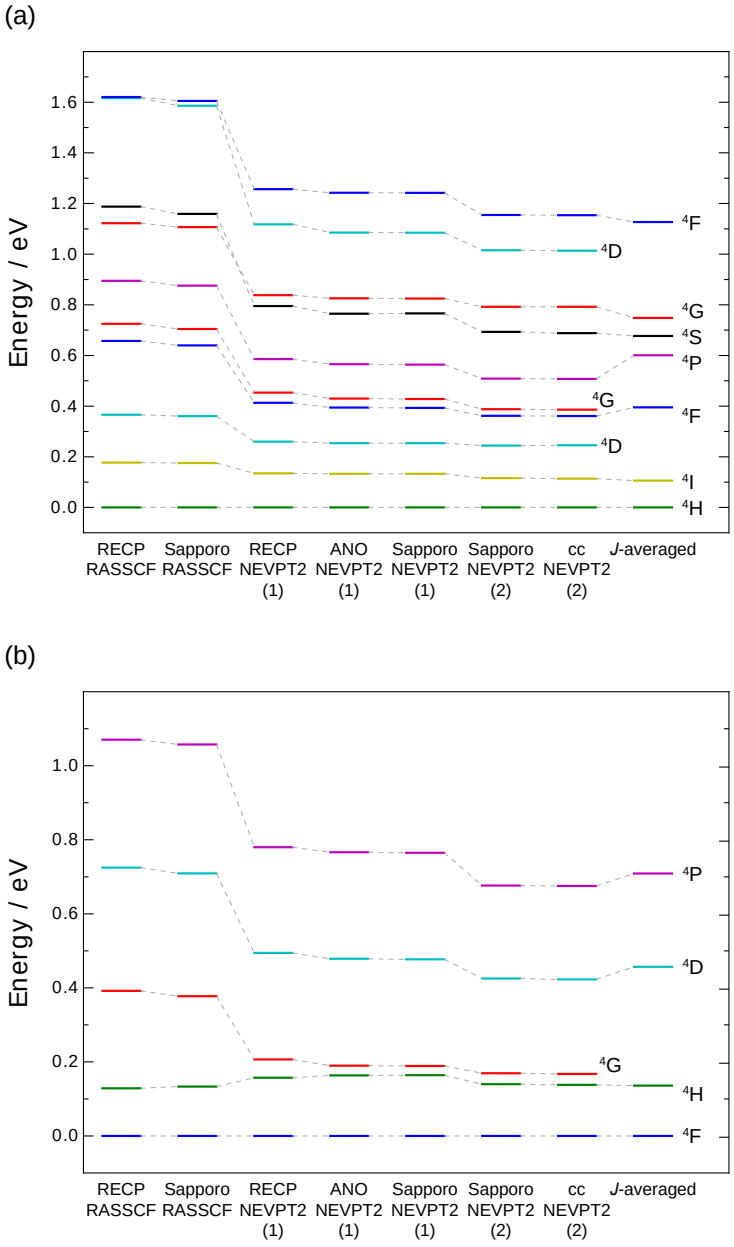

Figure 3-1. The calculated energy levels for the low-lying electronic states of Ce^{+} that originate from (a) the ground-state configuration, $[Xe]4f^{1}5d^{2}$, and (b) the excited-state configuration, $[Xe]4f^{1}5d^{1}6s^{1}$; the correlated orbitals in NEVPT2 calculations are (1) 4f, 5spd, and 6s and (2) 4spdf, 5spd, and 6s. The available experimental *J*-averaged values [13] are also shown.

Figure 3-1 shows the energy levels for (a) the electronic states of Ce^+, generated from the ground-state configuration, $[Xe]4f^15d^2$, and (b) those from the excited-state configuration, $[Xe]4f^15d^16s^1$, relative to the lowest electronic state of the respective configurations, calculated by the SA-RASSCF/NEVPT2 method with several basis sets. The *J*-averaged values calculated from available experimental data [13] are also given. As is shown in Figure 3-1, the energies of 70 states from the ground-state configuration are ranged within 1.2 eV, while those of 35 states from the excited-state configuration are ranged within 0.7 eV, indicating that a lot of electronic states are lying within a small energy range. As the results of the calculations, it is verified that the calculated energy levels have an appropriate degenerate feature in all computations, and thus, the respective atomic terms are indicated by a single line in Figure 3-1.

In Figure 3-1, the SA-RASSCF can almost reproduce the order of the electronic states for both ground-state and excited-state configurations from the experiment (only ^4S and ^4G states from the ground-state configuration are inconsistent with the experiment), although the excitation energies are overestimated in most cases. The NEVPT2 improves the SA-RASSCF energetics drastically, and the calculated excitation energies are in good agreement with the corresponding experimental values. In the NEVPT2 calculations, two different correlated orbital sets were employed, i.e., (1) 4f, 5spd, and 6s (RECP/def2-QZVPP, ANO-RCC, and Sapporo-DKH3-QZP-2012) and (2) 4spdf, 5spd, and 6s (Sapporo-DKH3-QZP-2012 and cc-pwCVQZ), and the comparison of these two different calculations shows that, at least, the electron correlation from 4f, 5spd, and 6s electrons needs to be included for quantitative discussions of the energetics, and that the dynamic

correlation effects due to the inner-shell 4spd electrons reduce the excitation energies slightly, resulting in better agreement with the experimental values. The energy levels of the ^{4}F and ^{4}S states from the ground-state configuration are much improved by the inner-shell electron correlation effect, while the ^{4}P state from the ground-state configuration shows a slightly large difference between the NEVPT2 value and experimental value. This difference may be ascribed to the *J*-averaged scheme from the experimental raw data, which do not consider the contributions from the other spin states.

The all-electron and RECP calculations show very similar energetics for the excitation energies, and thus, it is concluded that the all-electron and RECP basis sets employed in this study have a superior performance at the respective computational levels. The NEVPT2 calculations with the Sapporo-DKH3-QZP-2012 and cc-pwCVQZ basis sets (including 4spdf, 5spd, and 6s as correlated orbitals) show a similar accuracy in the energetics. The number of basis functions in the Sapporo-DKH3-QZP-2012 and cc-pwCVQZ basis sets are 222 and 282, respectively, and thus Sapporo-DKH3-QZP-2012 is a more compact and more efficient basis set. Table 3-1 shows the CPU times for each step of molecular integral, spin-restricted Hartree-Fock (RHF), SA-RASSCF, and NEVPT2 (for one state) computations, using four different basis sets. The computational time for SA-RASSCF increases as the number of basis function grows, but as to the computations for the molecular integral, Sapporo-DKH3-QZP-2012 shows a shorter CPU time than ANO-RCC. This is because Sapporo-DKH3-QZP-2012 was developed by a segmented contraction scheme, while the other basis sets were developed by a general contraction scheme. On the other hand, the NEVPT2 calculation with a strongly-

contracted scheme shows almost the same CPU time for any all-electron basis sets, since the correlation energy is estimated on the basis of the density matrix from the SA-RASSCF calculation [22]. In the following discussions, I employed the Sapporo-DKH3-QZP-2012 basis set that is compact and provides an equivalently accurate result to the cc-pwCVQZ basis set.

Table 3-1. The CPU times (in second) for molecular integral, RHF, SA-RASSCF, and one-state NEVPT2 computations, measured on a single-node computer equipped with one Intel Xeon W3690 (3.46 GHz) processor using one CPU core, using four different basis sets. The number in parenthesis after the basis set denotes the number of basis functions.

	integral	RHF	SA-RASSCF	NEVPT2
RECP (100)	6.2	0.3	3.5	355.4
ANO-RCC (192)	24.6	1.5	13.4	355.7
Sapporo-QZP (222)	22.9	2.1	19.1	358.8
cc-pwCVQZ (282)	147.0	5.6	37.8	382.6

Here, the relative energies for the electronic states derived from the ground-state configuration and those from the excited-state configuration are discussed. Figure 3-2 shows the calculated and experimental *J*-averaged energy levels of the related electronic states where the zero energy is set to the ground state. The energy difference of the lowest state with the $[Xe]4f^{1}5d^{2}$ configuration (^{4}H) and the lowest state with the $[Xe]4f^{1}5d^{1}6s^{1}$ configuration (^{4}F) was reported to be 0.209 eV in the experiment [13]. This small energy

difference suggests that the electronic states from the ground-state and excited-state configurations mix in with each other, and such a mixing can occur over the electronic states with the same symmetry representations. In the SA-RASSCF/NEVPT2 calculations for both $[Xe]4f^{1}5d^{2}$ and $[Xe]4f^{1}5d^{1}6s^{1}$ configurations, the SA-RASSCF orbitals were optimized with equally averaging ensembles originating from both configurations. The energy difference of the ^{4}H ($[Xe]4f^{1}5d^{2}$) and ^{4}F ($[Xe]4f^{1}5d^{1}6s^{1}$) states was calculated to be 0.292 eV, showing a slightly larger value than the experimental *J*-averaged value, 0.209 eV. To examine the mixing of the electronic states between these two configurations, I also investigated the CI coefficients of the SA-RASSCF wavefunction. Even in the most largely mixing case, the lowest and the second lowest ^{4}F states mix in with 2.0%, and the lowest and the second lowest ^{4}G states mix in with 0.025%, and thus, the mixing of these two configurations is not strong.

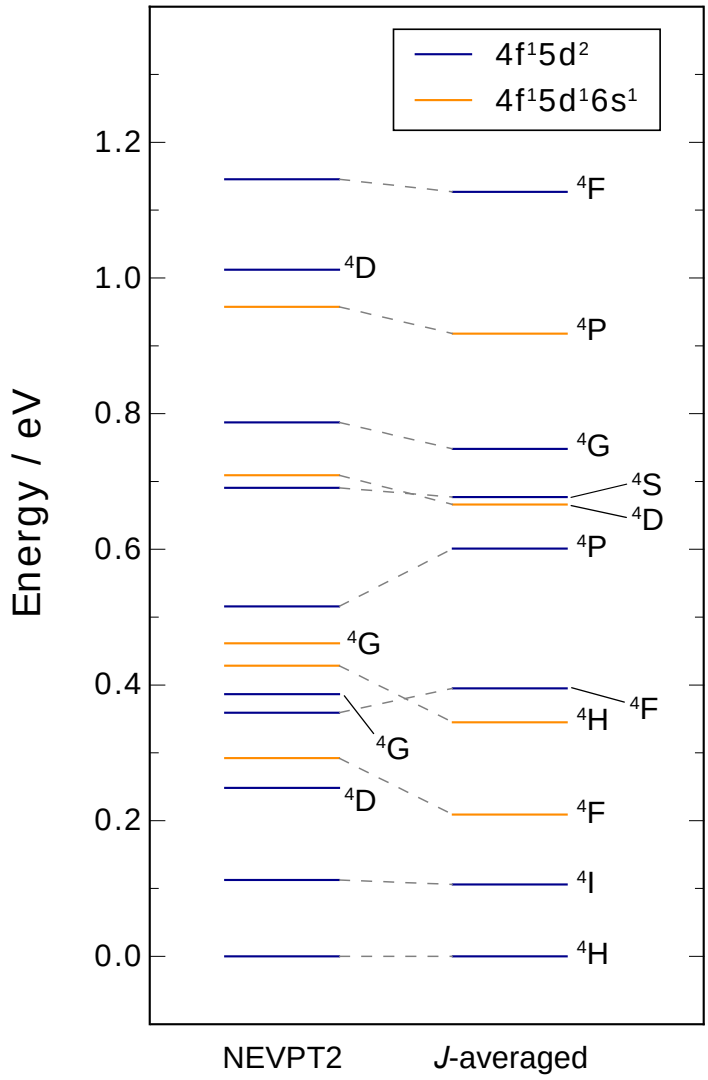

Figure 3-2. The comparison of the low-lying energy levels of Ce^{+} between the calculated (at SA-RASSCF/NEVPT2 with Sapporo-DKH3-QZP-2012) and *J*-averaged values calculated from the experimental data [13]. The electronic states shown here are only the quartet states derived from the ground-state configuration ($[Xe]4f^{1}5d^{2}$; in blue) and from the excited-state configuration ($[Xe]4f^{1}5d^{1}6s^{1}$; in orange).

Next, the energy levels of the spin-orbit coupled states of Ce^+ were calculated by the SOCI method. When considering only the quartet states, the number of independent states of the ground-state configuration ($[Xe]4f^15d^2$) amounts to 280 (= 70 × 4), while the number of independent electronic states of the excited-state configuration ($[Xe]4f^15d^16s^1$) amounts to 140 (= 35 × 4). Figure 3-3 shows the energy levels of the spin-orbit coupled states calculated from the ground-state configuration of quartet while Figure 3-4 shows those from the excited-state configuration of quartet at the SA-RASSCF and SA-RASSCF/NEVPT2 levels, as well as the available experimental energy levels [13]. As discussed above, the SA-RASSCF method tends to overestimate the excitation energies, while the NEVPT2 method reduces the excitation energies as a whole, approaching to the experimental values in the respective ensembles. The electronic states from the ground-state configuration lie within a range of 1.6 eV, while those from the excited-state configuration lie within a range of 1.0 eV.

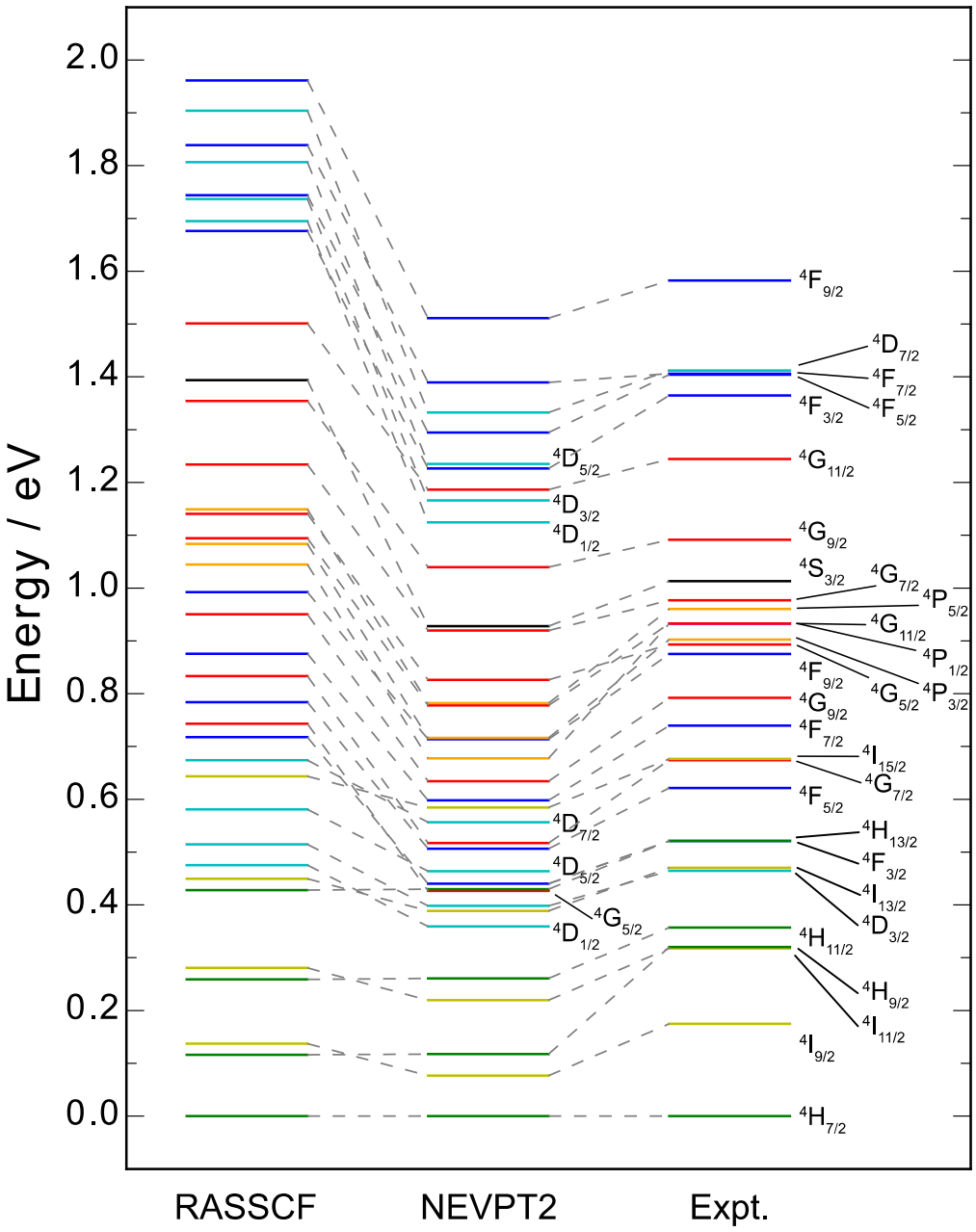

Figure 3-3. The SA-RASSCF, SA-RASSCF/NEVPT2, and experimental [13] energy levels of the ground and low-lying excited states of Ce^{+} which explicitly consider the spin-orbit coupling effects: the electronic states from the ground-state configuration ($[Xe]4f^{1}5d^{2}$).

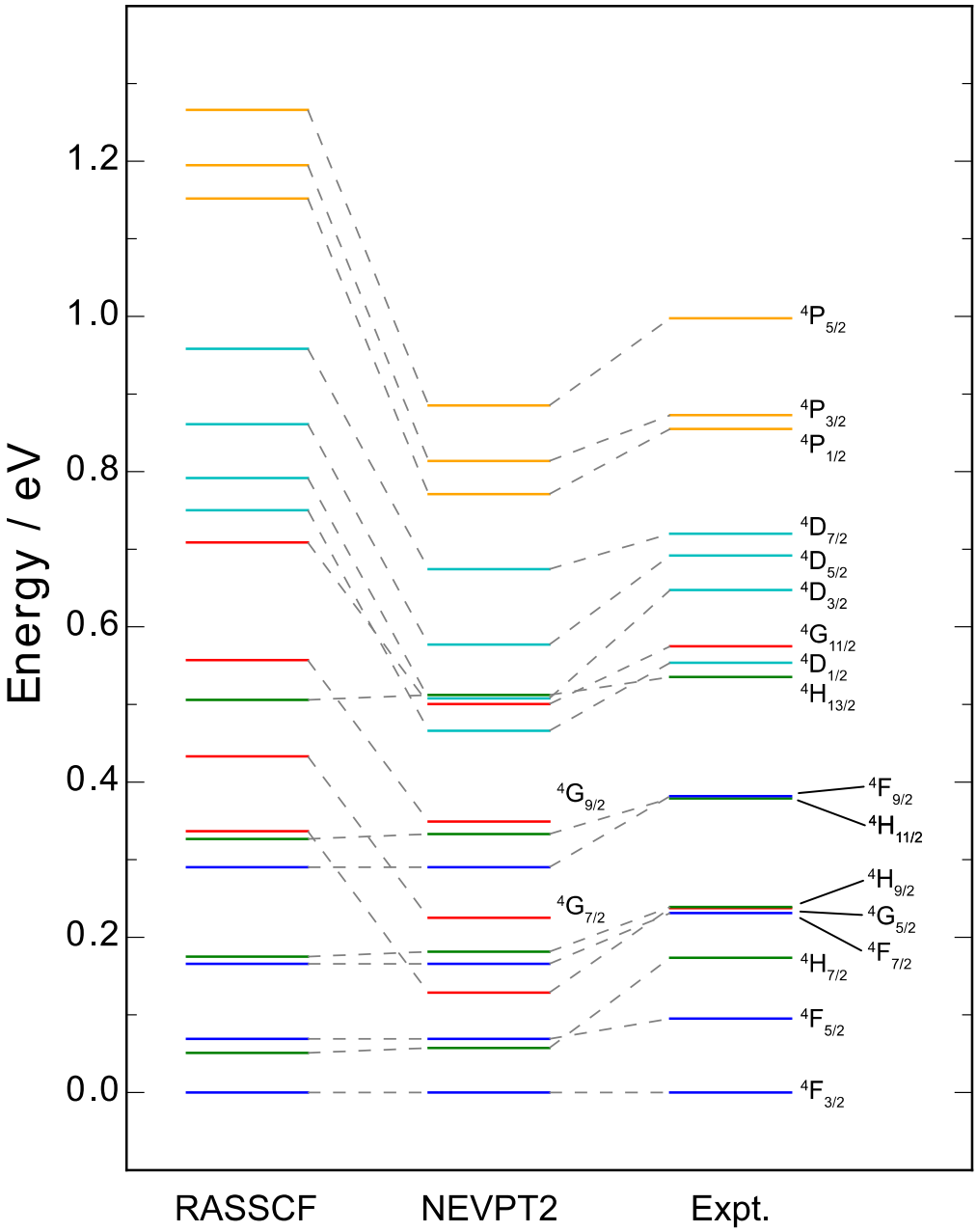

Figure 3-4. The SA-RASSCF, SA-RASSCF/NEVPT2, and experimental [13] energy levels of the ground and low-lying excited states of Ce^{+} which explicitly consider the spin-orbit coupling effects: the electronic states from the excited-state configuration ($[Xe]4f^{1}5d^{1}6s^{1}$).

In Figure 3-3 and Figure 3-4, qualitative agreement was obtained between the calculated and experimental energy levels, but in some cases the order in energy levels is different between the calculation and experiment. For example, in Figure 3-3, the energy level of the ^{4}P state is split to $^4P_{1/2}$, $^4P_{3/2}$, and $^4P_{5/2}$ by the spin-orbit coupling effect, and the order of the energy levels shows $E_{\mathrm{NEVPT2}}(^4P_{1/2}) < E_{\mathrm{NEVPT2}}(^4P_{3/2}) < E_{\mathrm{NEVPT2}}(^4P_{5/2})$, while experimentally the order was reported as $E_{\mathrm{exp}}(^4P_{3/2}) < E_{\mathrm{exp}}(^4P_{1/2}) < E_{\mathrm{exp}}(^4P_{5/2})$ [13]. This irregular order suggests the necessity to consider the contribution from the other spin states such as doublet, sextet, etc. It is noted that both the ground-state and excited-state configurations, [Xe]4f^{1}5d^2 and [Xe]4f^{1}5d^{1}6s^1, also generate an ensemble of doublet states with similar energies to the quartet states. To discuss the effect of a mixing from the doublet states, one needs to employ not SA-RASSCF but SA-CASSCF method in SOCI calculations due to a requirement of the MOLPRO program [17][18]. The employment of the SA-CASSCF method implies an appearance of many electronic states of different types of electronic configurations in the state-averaged solutions, and thus, I carried out SA-CASSCF calculations only for the quartet and doublet states originating from the ground-state configuration, [Xe]4f^{1}5d^2, by eliminating 6s orbital from the active space (only 4f and 5d are included in the active space), and in addition to the 280 (= 70 × 4) quartet states, only a part of the low-lying doublet states (^{2}G, ^{2}F, and ^{2}S) were involved in the SA-CASSCF/NEVPT2+SOCI calculations. The results are shown in Figure 3-5 where only the energy levels of the quartet-dominant electronic states are plotted. By including the doublet states, agreement between theory and experiment is drastically improved, especially in the lowest energy region. As for the order of $^4P_{1/2}$, $^4P_{3/2}$, and $^4P_{5/2}$

states mentioned above, the correct order is reproduced by including the spin-orbit coupling effects in Figure 3-5. The present results suggest the significance of an involvement of all the electronic states of spin multiplicities related to the target electronic configuration in the present SA-CASSCF/NEVPT2+SOCI approach. The same discussions will be given for CeF in the following chapter.

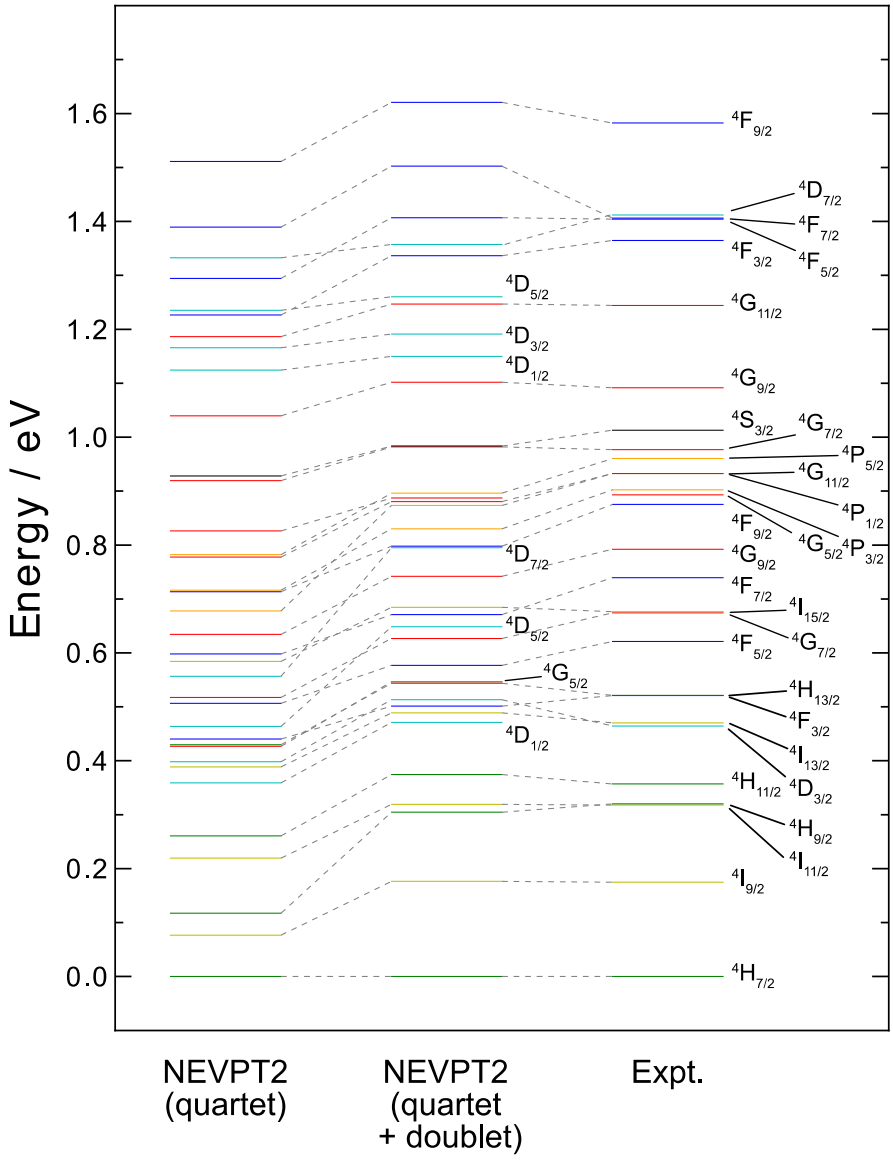

Figure 3-5. The NEVPT2 and experimental [13] energy levels of the ground and low-lying excited states of Ce^{+} which originate from the ground-state configuration ($[Xe]4f^{1}5d^{2}$). As for NEVPT2 results, two different calculated results are shown (SA-RASSCF/NEVPT2 for quartet and SA-CASSCF/NEVPT2 for quartet and doublet) where the energy levels in the left (NEVPT2 (quartet)) are the same as those of the middle one in Figure 3-3.

3.4 Conclusion

In this chapter, I performed a systematic calculation of the energy levels of the electronic states of Ce^+, which originate from the $4f^15d^16s^1$ and $4f^15d^2$ configurations, to examine the accuracy of *ab initio* computations based on all-electron and effective-core approaches. The significant factors for accurate computations of the electronic structures of the lanthanide element are the static and dynamic correlation effects, the scalar and spin-orbit relativistic effects, and the existence of multi-states within a small energy range due to an open-shell character with a high-spin multiplicity occupying 4f, 5d, and 6s orbitals. These complex factors require a state-of-the-art *ab initio* methodology including a good-quality basis set and a multi-configurational/multi-reference wavefunction. Noro developed all-electron basis set family, Sapporo-basis-set, which are also tested in this study. I carried out SA-RASSCF(SA-CASSCF)/NEVPT2 calculations without and with the spin-orbit coupling effects, for 420 electronic states of Ce^+, originating from $4f^15d^16s^1$ and $4f^15d^2$ quartet configurations. The mixing from doublet states through spin-orbit coupling was also examined, and it is shown that the inclusion of doublet-quartet mixing by spin-orbit coupling is essential to reproduce the energetics of the ground and low-lying excited states. Through comparisons with available experimental data, I decided to employ the SA-RASSCF(SA-CASSCF)/NEVPT2+SOCI method with the Sapporo-QZP basis set, and applied it to the CeF diatomic molecule in the next chapter.

3.5 References

[1] W. C. Elmler, R. B. Ross, and P. A. Christiansen, Adv. Quant. Chem., **19**, 139 (1988).

[2] E. Sanoyama, H. Kobayashi, and S. Yabushita, J. Mol. Struct. (Theochem), **451**, 189 (1998).

[3] T. Tsuchiya, T. Taketsugu, H. Nakano, and K. Hirao, J. Mol. Struct. (Theochem), **461**, 203 (1999).

[4] T. Nakajima and K. Hirao, Chem. Phys. Lett., **302**, 383 (1999).

[5] B. A. Hess, Phys. Rev. A, **33**, 3742 (1986).

[6] T. Nakajima, K. Hirao, J. Chem. Phys., **113**, 7786 (2000).

[7] M. Sekiya, T. Noro, T. Koga, and T. Shimazaki, Theor. Chem. Acc., **131**, 1247 (2012).

[8] B. O. Roos, R. Lindh, P.-Å. Malmqvist, V. Veryazov, P.-O. Widmark, and A. C. Borin, J. Phys. Chem. A, **112**, 11431 (2008).

[9] Q. Lu and K. A. Peterson, J. Chem. Phys., **145**, 54111 (2016).

[10] T. Noro, M. Sekiya, and T. Koga, Theor. Chem. Acc., **131**, 1124 (2012).

[11] T. Noro, M. Sekiya, and T. Koga, Theor. Chem. Acc., **132**, 1363 (2013).

[12] T. Noro, Segmented GTF basis set factory. http://sapporo.center.ims.ac.jp/sapporo/ (accessed December 8, 2017).

[13] W. C. Martin, R. Zalubas, and L. Hagan, Atomic Energy Levels: The Rare-Earth Elements (the Spectra of Lanthanum, Cerium, Praseodymium, Neodymium, Promethium, Samarium, Europium, Gadolinium, Terbium, Dysprosium, Holmium, Ebrium, Thulium, Ytterbium, and Lutetium), National Bureau of Standards, Washington, D.C. (1978).

[14] M. Dolg, H. Stoll, and H. Preuss, J. Chem. Phys., **90**, 1730 (1989).

[15] R. Gulde, P. Pollak, and F. Weigend, J. Chem. Theo. Comput., **8**, 4062 (2012).

[16] Wolf, M. Reiher, and B. A. Hess, J. Chem. Phys., **117**, 9215 (2002).

[17] H.-J. Werner, P. J. Knowles, G. Knizia, F. R. Manby, and M. Schütz, Wiley Interdisciplinary Reviews: Comput. Mol. Sci., **2**, 242 (2012).

[18] MOLPRO, version 2012.1, a package of *ab initio* programs, H.-J. Werner, P. J. Knowles, G. Knizia, F. R. Manby, M. Schütz, P. Celani, T. Korona, R. Lindh, A. Mitrushenkov, G. Rauhut, K. R. Shamasundar, T. B. Adler, R. D. Amos, A. Bernhardsson, A. Berning, D. L. Cooper, M. J. O. Deegan, A. J. Dobbyn, F. Eckert, E. Goll, C. Hampel, A. Hesselmann, G. Hetzer, T. Hrenar, G. Jansen, C. Köppl, Y. Liu, A. W. Lloyd, R. A. Mata, A. J. May, S. J. McNicholas, W. Meyer, M. E. Mura, A. Nicklass, D. P. O'Neill, P. Palmieri, D. Peng, K. Pflüger, R. Pitzer, M. Reiher, T. Shiozaki, H. Stoll, A. J. Stone, R. Tarroni, T. Thorsteinsson, and M. Wang, see http://www.molpro.net.

[19] J. Olsen, B. O. Roos, P. Jørgensen, and H. J. A. Jensen, J. Chem. Phys., **89**, 2185 (1988).

[20] C. Angeli, R. Cimiraglia, S. Evangelisti, T. Leininger, and J.-P. Malrieu, J. Chem. Phys., **114**, 10252 (2001).

[21] C. Angeli, R. Cimiraglia, and J. P. Malrieu, J. Chem. Phys., **117**, 9138 (2002).

[22] C. Angeli, M. Pastore, and R. Cimiraglia, Theor. Chem. Acc., **117**, 743 (2007).

[23] A. Berning, M. Schweizer, H.-J. Werner, P. J. Knowles, and P. Palmieri, Mol. Phys., **98**, 1823 (2000).

4. All-Electron Relativistic Spin-Orbit Computations on the Low-Lying Excited States and Spectroscopic Constants of CeF Diatomic Molecule

4.1 Introduction

The electronic structures of a series of low valency lanthanide monofluorides, LnF, have been known for a long time in the experimental community through the earlier work by the Gotkis group [1] and by the Field group [2][4]. The bonding nature of LnF is ionic where F^- is bound to Ln^+. The early lanthanide atom, Ce, has the ground-state configuration of $[Xe]4f^15d^16s^2$, while the Ce^+ ion has the ground-state configuration of $[Xe]4f^15d^2$ [5]. Interestingly, Ce^+ in the ground state of CeF has an electron configuration of $[Xe]4f^15d^16s^1$, which corresponds to the excited-state configuration of Ce^+ [2][3]. For CeF, two low-lying excited states were observed with excitation energies of 0.087 eV (Ω = 4.5) and 0.186 eV (Ω = 3.5) by selectively detected fluorescence excitation and dispersed fluorescence spectroscopy [4] where Ω denotes a quantum number for the total electronic angular momentum around the molecular axis (see Figure 2-1). To study the low-lying excited states and spectroscopic constants of CeF, Tatewaki and coworkers [6],[7] employed a four-component relativistic method with the single and double excitation configuration interaction (SDCI) and multi-configurational quasi-degenerate perturbation theory (MCQDPT), based on the reduced frozen-core approximation. In their calculations, good agreement with the experimental data was obtained for the Ce-F equilibrium bond length and stretching frequency, while the excitation energies were calculated to be 0.104 and 0.312 eV for the $\Omega = 4.5$ and $\Omega = 3.5$ states, respectively, which

are slightly larger than the corresponding experimental values (0.087 eV (Ω = 4.5) and 0.186 eV (Ω = 3.5)).

Very recently, Schoendorff and Wilson [8] employed the all-electron Sapporo-DKH3-TZP-2012 and Sapporo-TZP-2012 basis sets in the CASSCF and coupled-cluster calculations with an infinite order two-component method for the scalar relativistic effect to investigate the spectroscopic constants of the ground and low-lying excited states of lanthanide monofluorides, NdF and LuF. In their calculations, the significance of core correlation was verified to reproduce the bond dissociation energies. However, all-electron computations for the lanthanide compounds are still limited.

In this chapter, I report all-electron *ab initio* multiconfigurational/mutireference study on the ground and low-lying excited states of CeF, as well as the spectroscopic constants, based on a two-component relativistic scheme.

4.2 Computational Details

All-electron *ab initio* calculations were carried out for the ground and low-lying excited states of CeF, with all-electron relativistic basis sets, Sapporo-DKH3-QZP-2012 (13s11p9d7f4g3h1i) for Ce [9],[11] and Sapporo-QZP-2012 for F [10][11] (referred to as Sapporo-QZP), with the third-order Douglas-Kroll one-electron integrals [12] for the scalar relativistic effects. The target states are the nearly-degenerate low-lying quartet states of CeF in which the electronic structures of a Ce^+ part in CeF originate from the ground-state configuration, $[Xe]4f^15d^2$, and from the excited-state configuration, $[Xe]4f^15d^16s^1$. All the electronic structure calculations were carried out with the

Molpro2012 program package [13],[14].

The state-averaged restricted active space self-consistent field (SA-RASSCF) method [15] was employed for 70 quartet states of the $[Xe]4f^{1}5d^{2}$ configuration and 35 quartet states of the $[Xe]4f^{1}5d^{1}6s^{1}$ configuration separately, with the active space of 3 electrons in 13 orbitals. In the NEVPT2 calculations [16]-[18], 4spdf, 5spd, and 6s orbitals of Ce and 2sp orbitals of F were included as correlated orbitals. In the Breit–Pauli Hamiltonian scheme [19], the spin-orbit coupling matrix was generated for 280 electronic states (from the ground-state configuration with quartet) and for 140 electronic states (from the excited-state configuration with quartet) based on the SA-RASSCF wavefunction. Then, the SA-RASSCF energies for the respective electronic states in the diagonal terms were replaced with the corresponding NEVPT2 energies, followed by a diagonalization of the resultant spin-orbit coupling matrix to evaluate the energy levels of the spin-orbit-coupled states.

The energy levels of the excited states of CeF were calculated at the equilibrium structure by the SA-RASSCF/NEVPT2+SOCI approach. The additional calculations including doublet states were also performed by the SA-CASSCF/NEVPT2+SOCI approach. The Ce-F bond length and stretching frequency were evaluated by solving the one-dimensional rovibrational Schrödinger equation, using the VIBROT code in MOLCAS [20].

4.3 Results and Discussion

In Chapter 3, it was verified that the SA-CASSCF/NEVPT2+SOCI approach with the

Sapporo-DKH3-QZP-2012 basis sets can reproduce the energy levels of the low-lying electronic states of Ce^+ quantitatively, through a comparison with the experimental data. In this chapter, I first discuss the energy levels of the low-lying excited states of CeF calculated at SA-RASSCF/NEVPT2 with the Sapporo-QZP basis sets, followed by the SOCI calculation, to examine how the quasi-degenerate electronic states of Ce^+ change upon a formation of the CeF diatomic molecule. The bond length and vibrational frequency in the ground and excited states of CeF were also evaluated to discuss the accuracy of the present approach through a comparison with the available experimental data [4][21].

In a CeF diatomic molecule, F^- has a complete closed-shell configuration like a noble gas atom, and thus, the electronic structures of the Ce part in CeF are approximately represented by those of Ce^+, perturbed by F^-. Figure 4-1 shows the energy levels of those electronic states of $[Xe]4f^15d^16s^1$ and $[Xe]4f^15d^2$ configurations of Ce^+ (without SOCI) and CeF (without and with SOCI) where the energies are given relative to the lowest state of the respective species. In this calculation, the interatomic distance Ce-F was fixed at the experimental value, 2.048 Å [21], and 35 states from the $[Xe]4f^15d^16s^1$ configuration (shown in blue) and 70 states from the $[Xe]4f^15d^2$ configuration (shown in orange) were solved in a state-average scheme. It is known that, in CeF, the energies of the electronic states of the $[Xe]4f^15d^2$ configuration are raised up and $[Xe]4f^15d^16s^1$ becomes the ground-state configuration, although $[Xe]4f^15d^2$ is the ground-state configuration in the isolated Ce^+ [2],[3] (See Figure 4-2). This tendency was reproduced in the present calculations.

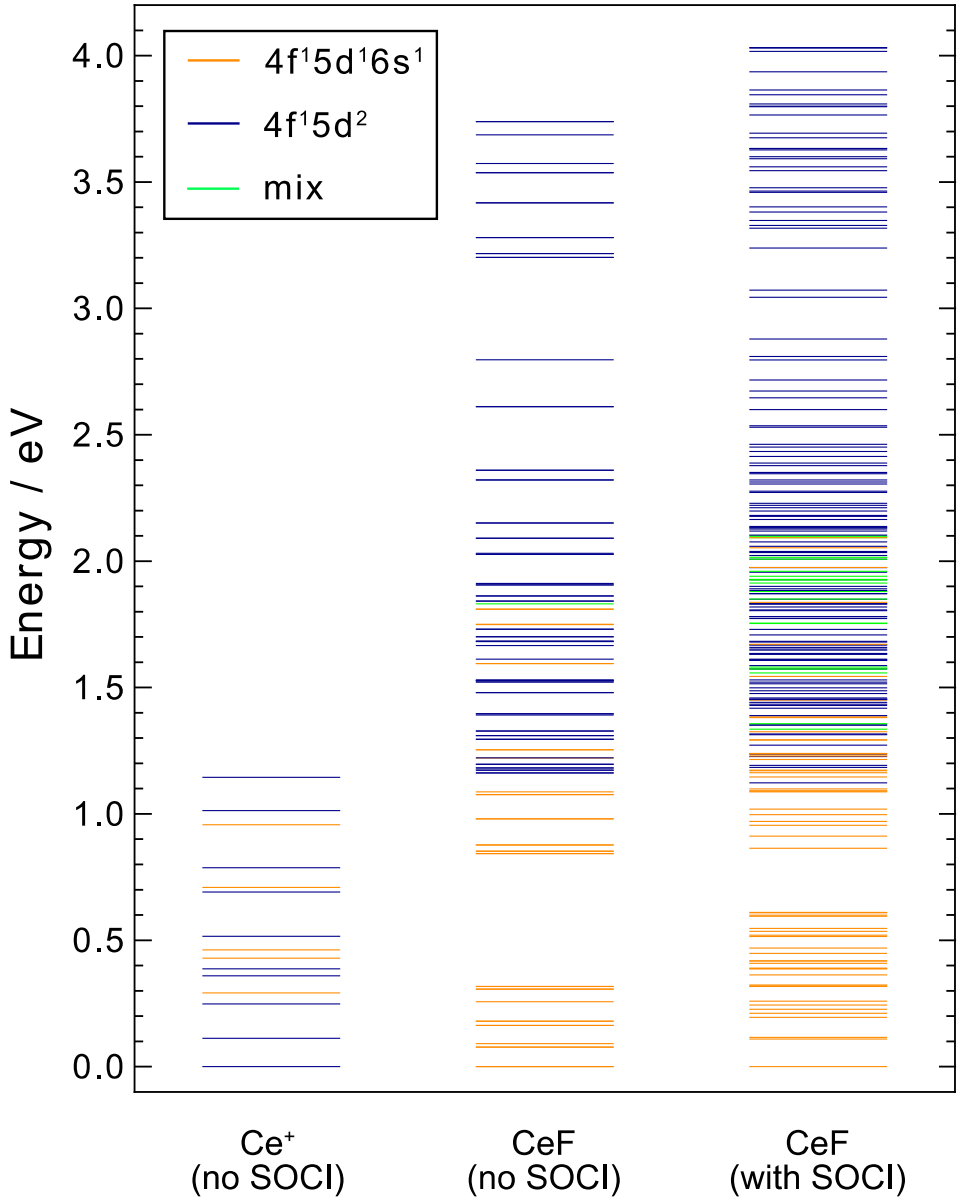

Figure 4-1. The energy levels of the low-lying electronic states of Ce^+ (without SOCI) and CeF (without and with SOCI), derived from the $[Xe]4f^15d^16s^1$ and $[Xe]4f^15d^2$ configurations of the Ce^+ part, calculated at the SA-RASSCF/NEVPT2 level with the Sapporo-QZP basis sets. The calculations for CeF were performed at the experimental bond length, r(Ce-F) = 2.048 Å [21].

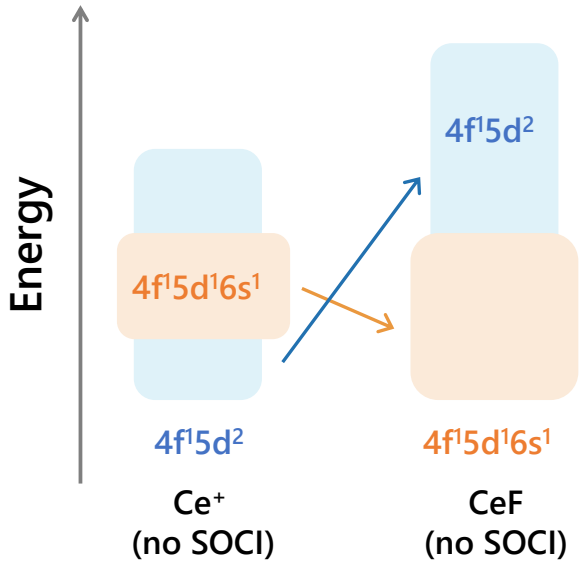

Figure 4-2. The schematic diagram for the change of the ground-state configuration in CeF, compared with Ce^+.

Hence, I discuss the origin of the change of the ground-state configuration from $[Xe]4f^15d^2$ in Ce^+ to $[Xe]4f^15d^16s^1$ in CeF. The difference in these two configurations is occupation numbers in 5d and 6s orbitals. In previous theoretical studies [1][6][7] contour maps of electron densities of the valence spinors in the ground state were shown for understanding of the electronic structure of CeF in which the 6p orbital mixes in the 6s spinor, resulting in an extension of the corresponding spinor to the other side from F^-. The same feature is observed in the present SA-RASSCF wavefunctions where the 6p orbital mixes in the singly-occupied 6s orbital (6s-6p hybridization), leading to the extension of the hybridized orbital to the backside of Ce^+ due to the Coulomb repulsion, as shown Figure 4-3. It is noted that 5d can also hybridize with p-type orbitals to represent a polarization, but the hybridization of 5d was small due to the energy difference between

5d and 6p. Thus, the electronic states of the $[Xe]4f^{1}5d^{1}6s^{1}$ configuration are relatively stabilized compared to those of the $[Xe]4f^{1}5d^{2}$ configuration.

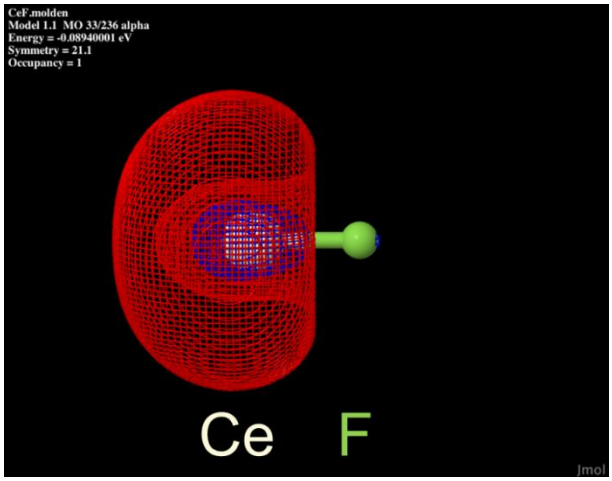

Figure 4-3. The molecular orbital for Ce-6s. The Coulomb repulsion from F^{-} can decrease by the 6s-6p hybridization where the electron in Ce-6s is able to extend to the other side of F^{-}.

As shown in Figure 4-1, 105 electronic states in Ce^{+} are lying very crowdedly in a range of 0–1.2 eV, whereas in CeF without SOCI, the energy range of these states expands largely, so that the electronic states of the $[Xe]4f^{1}5d^{1}6s^{1}$ configuration lie in a range of 0–1.8 eV while the electronic states of the $[Xe]4f^{1}5d^{2}$ configuration lie in a range of 1.2–3.8 eV. The state mixing between these two configurations occurs very rarely, and only one state shows a mixing of more than 30%, indicated by green line. In Figure 4-1, the electronic states from the $[Xe]4f^{1}5d^{1}6s^{1}$ configuration without SOCI (in orange) split to three groups with a range of 0–0.32 eV, 0.84–1.3 eV, and 1.6–1.8 eV. Figure 4-4 shows the three groups and this grouping is related to the magnetic quantum number of the occupied 5d orbital in $[Xe]4f^{1}5d^{1}6s^{1}$ configuration: $5d_{\pm 2}$ ($d_{x^2-y^2}$ or d_{xy}) in the lowest group,

$5d_{\pm1}$ (d_{xz} or d_{yz}) in the second lowest group, and $5d_0$ (d_{z^2}) in the highest group. This order of 5d orbitals can be understood by considering the Coulomb repulsion between F^- and an electron in 5d orbitals; due to a spatial distribution of 5d orbitals, the order in a repulsion force from F^- should be $5d_0 > 5d_{\pm1} > 5d_{\pm2}$. It should be noted that 4f-electron is lying closer to the nucleus than 5d-electron. The order of energy in the electronic states derived from the $[Xe]4f^15d^2$ configuration can also be explained by considering a spatial distribution of singly-occupied 5d orbitals.

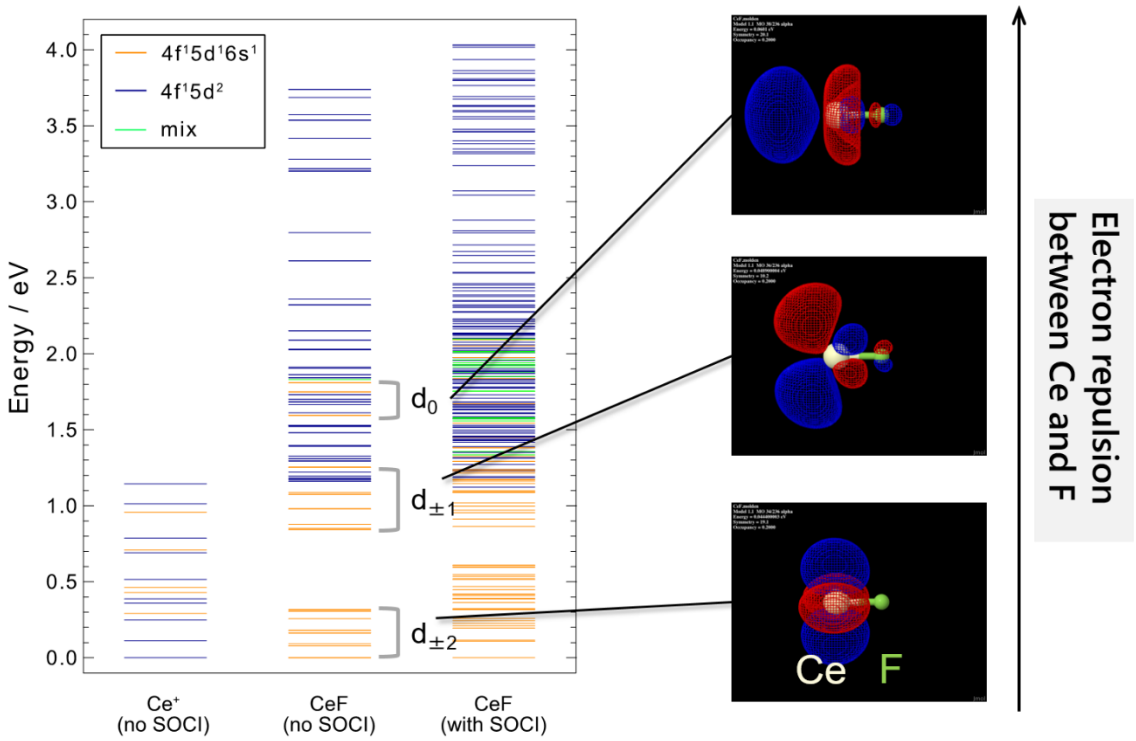

Figure 4-4. The comparison of the electronic states of Ce^+ (no SOCI) and CeF (no SOCI and with SOCI) with both the $[Xe]4f^15d^16s^1$ and $[Xe]4f^15d^2$ configurations. The electronic states with the configulation, $4f^15d^16s^1$, split into three groups according to the singly-occupied 5d orbitals.

Next, I compare the energy levels of the quartet states from the $[Xe]4f^{1}5d^{1}6s^{1}$ and $[Xe]4f^{1}5d^{2}$ configurations calculated for CeF without SOCI and with SOCI shown in Figure 4-1. The SOCI has brought a mixing of the spin-orbit uncoupled states of CeF, leading to more complexity of the electronic states. The number of the electronic states showing the mixing of $[Xe]4f^{1}5d^{1}6s^{1}$ and $[Xe]4f^{1}5d^{2}$ configurations (indicated by green lines) increases to 20. There are 420 (= 105 × 4) independent electronic states originating from quartet states for CeF in a range of 0–4 eV where 56 electronic states in the lowest-lying region (0–0.62 eV) derived by the SOCI calculations correspond to those of the $[Xe]4f^{1}5d_{\pm2}{}^{1}6s^{1}$ configuration.

Hence, I focus on this lowest-lying energy region of CeF, and carried out SA-RASSCF/NEVPT2+SOCI calculations for the 56 states (originating from quartet states). In addition, I carried out SA-CASSCF/NEVPT2+SOCI calculations for the 56 states originating from quartet states and the 46 states originating from doublet states, to examine the mixing of quartet and doublet states via spin-orbit coupling effects. The number of the doublet states included was determined through a preliminary calculation where the lowest 46 states are lying in a range of 0–0.62 eV at the SA-CASSCF/NEVPT2 level. Figure 4-5 shows the energy levels calculated by SA-RASSCF/NEVPT2+SOCI for only quartet states and by SA-CASSCF/NEVPT2+SOCI for both quartet and doublet states, as well as the available experimental data [4] and previously calculated results by the four-component relativistic scheme with the MCQDPT method [7]. In Figure 4-5, the respective electronic states of CeF are distinguished by Ω (quantum number for the total electronic angular momentum around the molecular axis, see Figure 2-1). Experimentally,

the ground state of CeF was assigned as Ω = 3.5, and the excitation energies for the electronic states of Ω = 4.5 and 3.5 were reported to be 0.087 and 0.186 eV, respectively [4]. The corresponding values in the present SA-RASSCF/NEVPT2+SOCI calculations for only quartet are 0.116 eV (Ω = 4.5) and 0.211 eV (Ω = 3.5), which are in good agreement with the experimental data. By including the mixing with the doublet states in the SOCI calculations, these values are reduced to 0.104 eV (Ω = 4.5) and 0.155 eV (Ω = 3.5), and thus, the former value is in better agreement with the experiment, while the latter show a similar deviation (0.03 eV) from the experiment. The previous four-component relativistic MCQDPT calculations based on the CASCI wavefunction estimated the corresponding energies to be 0.104 eV (Ω = 4.5) and 0.312 eV (Ω = 3.5), and thus, the energy level of the latter state of Ω = 3.5 was overestimated by twice [7]. In their study, only the electronic states of Ω = 1.5, 2.5, 3.5, and 4.5 were calculated to avoid the intruder states, and thus, their result looks sparse compared to the present calculations. The present SA-CASSCF/NEVPT2+SOCI calculations show that the ratio of quartet and doublet in the spin-orbit coupled states are 0.986 : 0.014 (the ground state), 0.953 : 0.047 (the excited state with Ω = 4.5), and 0.898 : 0.102 (the excited state with Ω = 3.5), and thus, the mixing from doublet is not so large in these observed states.

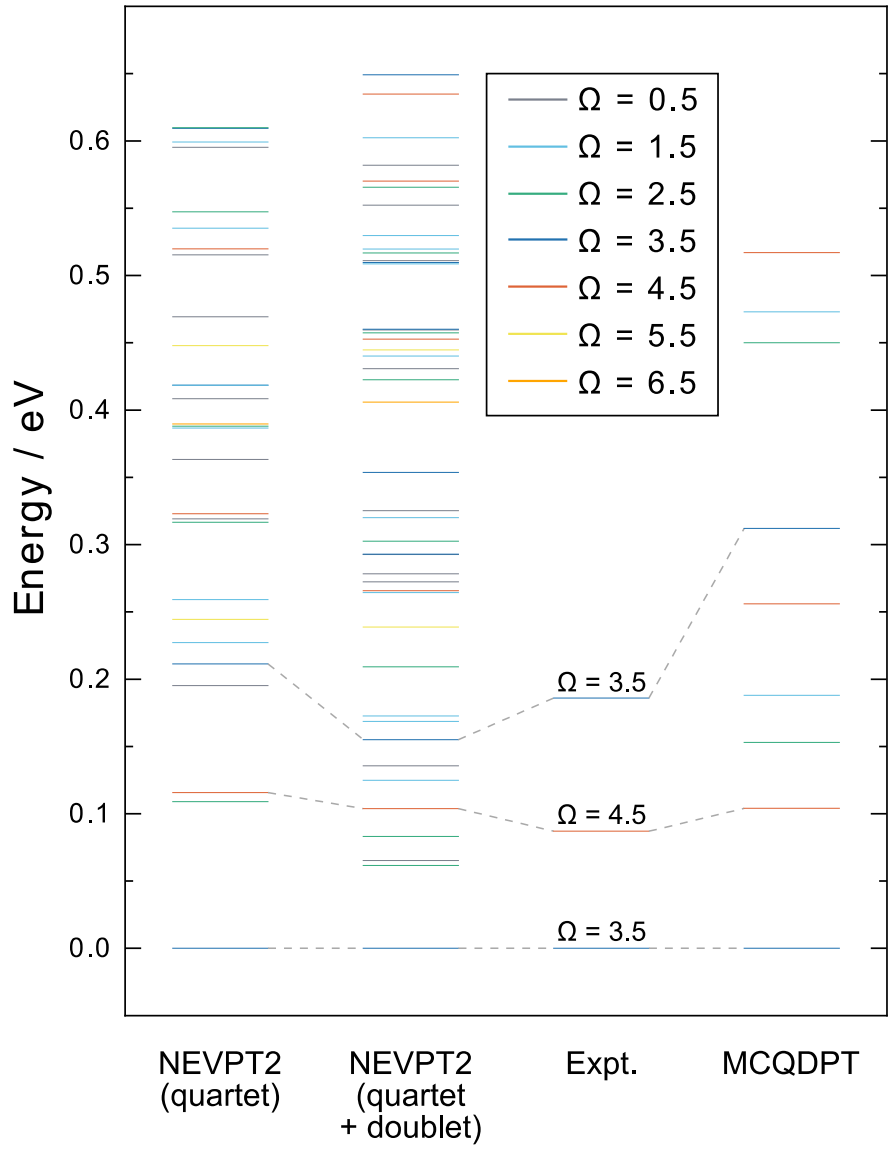

Figure 4-5. The energy levels of the low-lying electronic states of CeF with the $[Xe]4f^{1}5d^{1}6s^{1}$ configuration at the experimental bond length, r(Ce-F) = 2.048 Å [21], calculated by SA-RASSCF/NEVPT2+SOCI for quartet and by SA-CASSCF/NEVPT2+SOCI for quartet and doublet. The available experimental data [4] and previous theoretical results by the four-component relativistic method with MCQDPT [7] are also shown.

Finally, the bond length and stretching frequency were calculated for CeF at the SA-RASSCF/NEVPT2+SOCI (for the 56 states from quartet) and SA-CASSCF/NEVPT2+SOCI (for the 56 states from quartet and the 46 states from doublet) levels. In the respective computational levels, the potential energy curves were generated from single-point energy calculations around the equilibrium distance, i.e., in a range of r(Ce-F) = 1.9–2.2 Å with a step of 0.01 Å, and the low-lying rovibrational states were calculated for the ground (Ω = 3.5) and excited (Ω = 4.5) states by numerically solving the rovibrational Schrödinger equation using the MOLCAS program [20]. Table 4-1 summarizes the calculated bond lengths and stretching frequencies for CeF with the available experimental data [4][21]. The bond length for the zero-point vibrational state, r_0, is calculated from the corresponding rotational constant, B_0, for $^{140}Ce^{19}F$ in both present calculations and the experiment. In the SA-RASSCF/NEVPT2+SOCI (for quartet) calculations for the ground state, the anharmonicity lengthens the Ce-F bond as r_e = 2.0322 Å to r_0 = 2.0346 Å, and reduces the Ce-F frequency as ν_e = 557.8 cm^{-1} to ν_0 = 554.0 cm^{-1}, and thus, the anharmonicity is not so strong. The calculated bond lengths are shorter by 0.013 Å than the corresponding experimental values, and the calculated stretching frequencies are larger by 10 cm^{-1} than the corresponding experimental values. In the SA-RASSCF/NEVPT2+SOCI (for quartet) calculations for the excited state (Ω = 4.5), the bond length slightly shortens while the vibrational frequency slightly increases, and this tendency is very consistent with the experimental data. By including the mixing from doublet states, the Ce-F bond length slightly decreases, and the Ce-F stretching frequency slightly increases in both electronic states, and thus, the deviation of the

calculated values and the experimental ones becomes slightly large. It is noted that in the ground state and the target excited state with Ω = 4.5, the mixing weight from doublet states is very small (0.01–0.05) as described above, and thus, the mixing with double states in SOCI calculations works to make the calculated spectroscopic constants worse, since the weight for the target states in the state-average scheme in SA-CASSCF becomes smaller.

Table 4-1. The bond length (equilibrium (r_e) and zero-point vibrational state (r_0)), and the vibrational frequency (harmonic one (ν_e) and fundamental one (ν_0)) of CeF for the ground state (Ω = 3.5) and the excited state (Ω = 4.5), calculated at the SA-RASSCF/NEVPT2+SOCI (for the 56 states from quartet) and SA-CASSCF/ NEVPT2+SOCI (for the 56 states from quartet and the 46 states from doublet) levels, with the available experimental data.

	r_e (Å)	r_0 (Å)	ν_e (cm^{-1})	ν_0 (cm^{-1})
Ground state (Ω = 3.5)				
NEVPT2 (quartet)	2.0322	2.0346	557.8	554.0
NEVPT2 (quartet+doublet)	2.0313	2.0338	560.1	558.1
Expt.[4,21]	–	2.0478	–	543.76
Excited state (Ω = 4.5)				
NEVPT2 (quartet)	2.0311	2.0335	558.1	554.2
NEVPT2 (quartet+doublet)	2.0287	2.0316	558.9	558.6
Expt.[4]	–	2.0471	–	544

4.4 Conclusion

In this chapter, I summarized the results of a systematic calculation of the energy levels of the electronic states of CeF, which originate from the $4f^{1}5d^{1}6s^{1}$ and $4f^{1}5d^{2}$ configurations of Ce^{+}. Following the detailed calculations for Ce^{+} in Chapter 3, I employed SA-RASSCF(SA-CASSCF)/NEVPT2+SOCI approach with the Sapporo all-electron relativistic basis sets, to calculate the ground and low-lying excited states (420 electronic states), originating from $4f^{1}5d^{1}6s^{1}$ and $4f^{1}5d^{2}$ quartet configurations of Ce^{+}. The excitation energies, the equilibrium bond length, and the vibrational frequency are well reproduced by the present computations.

4.5 References

[1] I. Gotkis, J. Phys. Chem., **95**, 6086 (1991).

[2] L. A. Kaledin, C. Linton, T. E. Clarke, and R. W. Field, J. Mol. Spectrosc., **154**, 417 (1992).

[3] L. Kaledin, M. C. Heaven, R. W. Field, and L. A. Kaledin, J. Mol. Spectrosc., **179**, 310 (1996).

[4] J. C. Bloch, M. C. McCarthy, R. W. Field, and L. A. Kaledin, J. Mol. Spectrosc., **177**, 251 (1996).

[5] W. C. Martin, R. Zalubas, and L. Hagan, Atomic Energy Levels: The Rare-Earth Elements (the Spectra of Lanthanum, Cerium, Praseodymium, Neodymium, Promethium, Samarium, Europium, Gadolinium, Terbium, Dysprosium, Holmium, Ebrium, Thulium, Ytterbium, and Lutetium), National Bureau of Standards, Washington, D.C. (1978).

[6] Y. Wasada-Tsutsui, Y. Watanabe, and H. Tatewaki, J. Phys. Chem. A, **111**, 8877 (2007).

[7] H. Tatewaki, S. Yamamoto, Y. Watanabe, and H. Nakano, J. Chem. Phys., **128**, 214901 (2008).

[8] G. Schoendorff and A. K. Wilson, J. Chem. Phys., **140**, 224314 (2014).

[9] M. Sekiya, T. Noro, T. Koga, and T. Shimazaki, Theor. Chem. Acc., **131**, 1247 (2012).

[10] T. Noro, M. Sekiya, and T. Koga, Theor. Chem. Acc., **131**, 1124 (2012).

[11] T. Noro, Segmented GTF basis set factory, http://sapporo.center.ims.ac.jp/sapporo/ (accessed December 8, 2017).

[12] A. Wolf, M. Reiher, and B. A. Hess, J. Chem. Phys., **117**, 9215 (2002).

[13] H.-J. Werner, P. J. Knowles, G. Knizia, F. R. Manby, and M. Schütz, Wiley Interdisciplinary Reviews: Comput. Mol. Sci., **2**, 242 (2012).

[14] MOLPRO, version 2012.1, a package of *ab initio* programs, H.-J. Werner, P. J. Knowles, G. Knizia, F. R. Manby, M. Schütz, P. Celani, T. Korona, R. Lindh, A. Mitrushenkov, G. Rauhut, K. R. Shamasundar, T. B. Adler, R. D. Amos, A. Bernhardsson, A. Berning, D. L. Cooper, M. J. O. Deegan, A. J. Dobbyn, F. Eckert, E. Goll, C. Hampel, A. Hesselmann, G. Hetzer, T. Hrenar, G. Jansen, C. Köppl, Y. Liu, A. W. Lloyd, R. A. Mata, A. J. May, S. J. McNicholas, W. Meyer, M. E. Mura, A. Nicklass, D. P. O'Neill, P. Palmieri, D. Peng, K. Pflüger, R. Pitzer, M. Reiher, T. Shiozaki, H. Stoll, A. J. Stone, R. Tarroni, T. Thorsteinsson, and M. Wang, see http://www.molpro.net.

[15] J. Olsen, B. O. Roos, P. Jørgensen, and H. J. A. Jensen, J. Chem. Phys., **89**, 2185 (1988).

[16] C. Angeli, R. Cimiraglia, S. Evangelisti, T. Leininger, and J.-P. Malrieu, J. Chem. Phys., **114**, 10252 (2001).

[17] C. Angeli, R. Cimiraglia, and J. P. Malrieu, J. Chem. Phys., **117**, 9138 (2002).

[18] C. Angeli, M. Pastore, and R. Cimiraglia, Theor. Chem. Acc., **117**, 743 (2007).

[19] A. Berning, M. Schweizer, H.-J. Werner, P. J. Knowles, and P. Palmieri, Mol. Phys., **98**, 1823 (2000).

[20] F. Aquilante, L. De Vico, N. Ferré, G. Ghigo, P.-Å. Malmqvist, P. Neogrády, T. B. Pedersen, M. Pitoňák, M. Reiher, B. O. Roos, L. Serrano-Andrés, M. Urban, V. Veryazov, and R. Lindh, J. Comput. Chem., **31**, 224 (2010).

[21] Y. Azuma, W. J. Childs, and K. L. Menningen, J. Mol. Spectrosc., **145**, 413 (1991).

5. All-Electron Relativistic Spin-Orbit Computations on the Low-Lying Excited States and Spectroscopic Constants of CeH Diatomic Molecule

5.1 Introduction

I move to the next target molecule, CeH. In a case of CeF, the bonding nature is almost a pure ionic bond between Ce^{+} and F^{-}, while in CeH, a covalent nature should appear between a Ce atomic orbital and H-1s orbital. The ground-state electronic structure of Ce atom is $[Xe]4f^{1}5d^{1}6s^{2}$ where 4f orbitals are contracted inside, and so H-1s orbital will make a bond with 5d orbital of Ce. As a previous theoretical study, Dolg et al. [1] examined the bond length and vibrational frequency of CeH in the lowest doublet state, using RECP. Wilson and Andrews performed a combined study of matrix-isolation spectroscopy and DFT calculations on these systems, in which only a quartet state was examined for CeH [2]. In 2009, Goto, Noro, and Taketsugu studied the energy levels of the low-lying doublet and quartet states of CeH by B3LYP, CCSD(T), and CASPT2 methods [3]. B3LYP calculations were performed with the Stuttgart-Köln RECP, while *ab initio* all-electron calculations at the CASPT2 and CCSD(T) levels were performed with the TZP basis sets [4][5] and the second-order Douglas-Kroll scheme [6], using MOLPRO2006 program [7]. In their CASPT2 calculations, the numbers of target electronic states of CeH were seven and eleven for doublet and quartet, respectively, and the spin-orbit coupling effects were considered only for the respective doublet and quartet ensembles. DFT and CCSD(T) calculations showed the ground state of CeH to be doublet,

while CASPT2 calculations showed the ground state to be quartet. Analyses of electronic wavefunctions show that both quartet and doublet states have a multi-configurational character, and so they cannot be described by the single-configuration based methods, CCSD(T) and DFT. In Goto's CASPT2 calculations, however, there remains an inconsistency between theory and experiment in which the Ce-H stretching frequency is overestimated, and more sophisticated theoretical computations are required to solve this inconsistency.

In this chapter, I apply the formulation of all-electron *ab initio* multiconfigurational/mutireference approach with the Sapporo basis sets based on a two-component relativistic scheme to the lowest-lying doublet and quartet states of CeH. I will determine the ground states of CeH to be doublet or quartet by considering the static and dynamic correlation effects, scalar and spin-orbit relativistic effects, and quasi-degenerate multi-state features, appropriately. The equilibrium bond length and vibrational frequency of CeH are also calculated based on the potential energy curves for doublet and quartet states, which will be compared with the experimental data.

5.2 Computational Details

All-electron *ab initio* calculations were carried out for the ground and low-lying excited states of CeH, with all-electron relativistic basis sets, Sapporo-DKH3-QZP-2012 (13s11p9d7f4g3h1i) for Ce [8][10] and Sapporo-QZP-2012 for H [9][10] (referred to as Sapporo-QZP), with the third-order Douglas-Kroll one-electron integrals [6] for the scalar relativistic effects. The target electronic states are the nearly-degenerate lowest-

lying quartet (^{4}H) and doublet (^{2}F) states of CeH in which the electronic configurations are expected to be $4f^1 5d^1 (5d_\sigma\text{-}H_{1s})^2 6s^1$ and $4f^1 (5d_\sigma\text{-}H_{1s})^2 6s^2$, respectively, from previous calculations [3]. All the electronic structure calculations were carried out with the MOLPRO2012 program package [11][12].

The SA-CASSCF method [13] was employed for 11 quartet and 7 doublet states with the active space of 5 electrons in 14 orbitals (Ce-4f, 5d, 6s, and H-1s). In the NEVPT2 calculations [14][16], 4spdf, 5spd, and 6s orbitals of Ce and H-1s orbitals were included as correlated orbitals. In the Breit–Pauli Hamiltonian scheme [17], the spin-orbit coupling matrix was generated based on the SA-CASSCF wavefunction, and then, the SA-CASSCF energies for the respective electronic states in the diagonal terms were replaced with the corresponding NEVPT2 energies, followed by a diagonalization of the resultant spin-orbit coupling matrix to evaluate the energy levels of the spin-orbit-coupled states.

The energy levels of the excited states of quartet and doublet were calculated for CeH at r(Ce-H) = 2.0 Å that is close to the equilibrium bond length, by the SA-CASSCF/NEVPT2+SOCI approach. The Ce-H bond length and stretching frequency were evaluated by solving the one-dimensional rovibrational Schrödinger equation, using the VIBROT code in MOLCAS [18].

5.3 Results and Discussion

In the present SA-CASSCF/NEVPT2 calculations, a state-average scheme was applied to 11 quartet and 7 doublet states, assuming that the lowest-lying quartet is ^{4}H

($4f^1 5d^1(5d_\sigma\text{-}H_{1s})^2 6s^1$), while the lowest-lying doublet is ^2F ($4f^1(5d_\sigma\text{-}H_{1s})^2 6s^2$), based on the previous DFT and CCSD(T) calculations [3]. However, the present calculations show that the lowest-lying electronic state is $4f^1 5d^1(5d_\sigma\text{-}H_{1s})^2 6s^1$ in both quartet and doublet. The energy difference of doublet and quartet is very small, and the spin multiplicity of the ground state changes depending on the computational levels. Figure 5-1 shows the energy levels of the lowest quartet and doublet states calculated by the SA-CASSCF method without and with SOCI calculations, and SA-CASSCF/NEVPT2 method without and with SOCI calculations, where the energy level of the lower state is set to be zero in the respective computational levels. In this calculation, the interatomic distance Ce-H was fixed at 2.0 Å which is closes to the equilibrium distance. At the SA-CASSCF level without SOCI, the ground state is quartet, with the doublet state lying 0.070 eV high; by including the spin-orbit coupling effect, their energy difference becomes larger (0.233 eV), since the spin-orbit coupling effect lowers the quartet state more than the doublet state. It is noted that SOCI calculations mix the quartet and doublet states, and the weight of quartet state in the ground state is 90%, while the weight of the doublet state at 0.233 eV is only 26.4% (there are excited states with the larger weight of doublet states in a higher energy region). By including dynamic correlation effect through NEVPT2 calculation, the doublet becomes the ground state, while additional spin-orbit coupling effect changes the ground state to be quartet, with the doublet state lying 0.100 eV high. In the SA-CASSCF/NEVPT2+SOCI results, the weight of quartet state in the ground state is 81.3%, while the weight of the doublet state at 0.100 eV is only 43.1%. It is concluded that the ground state of CeH is $^4H_{7/2}$ due to the dynamic correlation and spin-

orbit coupling effects.

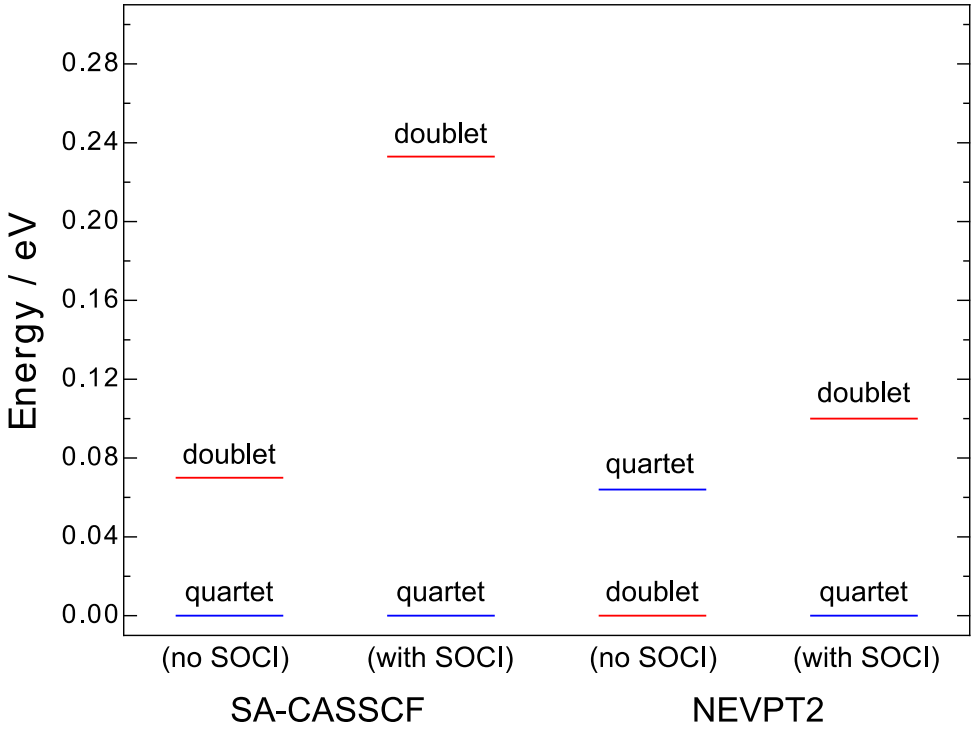

Figure 5-1. The energy levels of the lowest quartet (in blue) and doublet (in red) states of CeH at *r*(Ce-H) = 2.00 Å, calculated by SA-CASSCF (without and with SOCI) and SA-CASSCF/NEVPT2 (without and with SOCI).

Figure 5-2 shows the potential energy curves for low-lying five electronic states, generated from single-point energy calculations around the equilibrium distance, i.e., in a range of *r*(Ce-H) = 1.85–2.25 Å with a step of 0.05 Å. For the single-point energy calculations, the SA-CASSCF/NEVPT2+SOCI calculations were performed. It is shown that in the low-lying energy region, there are five electronic states with Ω = 3.5, 0.5, 1.5, 4.5, and 2.5, and only the state with Ω = 2.5 has contributions from doublet states (other states are almost quartet states). he potential energy profile for Ω = 2.5 (doublet) is clearly

different from the other profiles (quartet); the doublet state has the shorter equilibrium bond length than the quartet states.

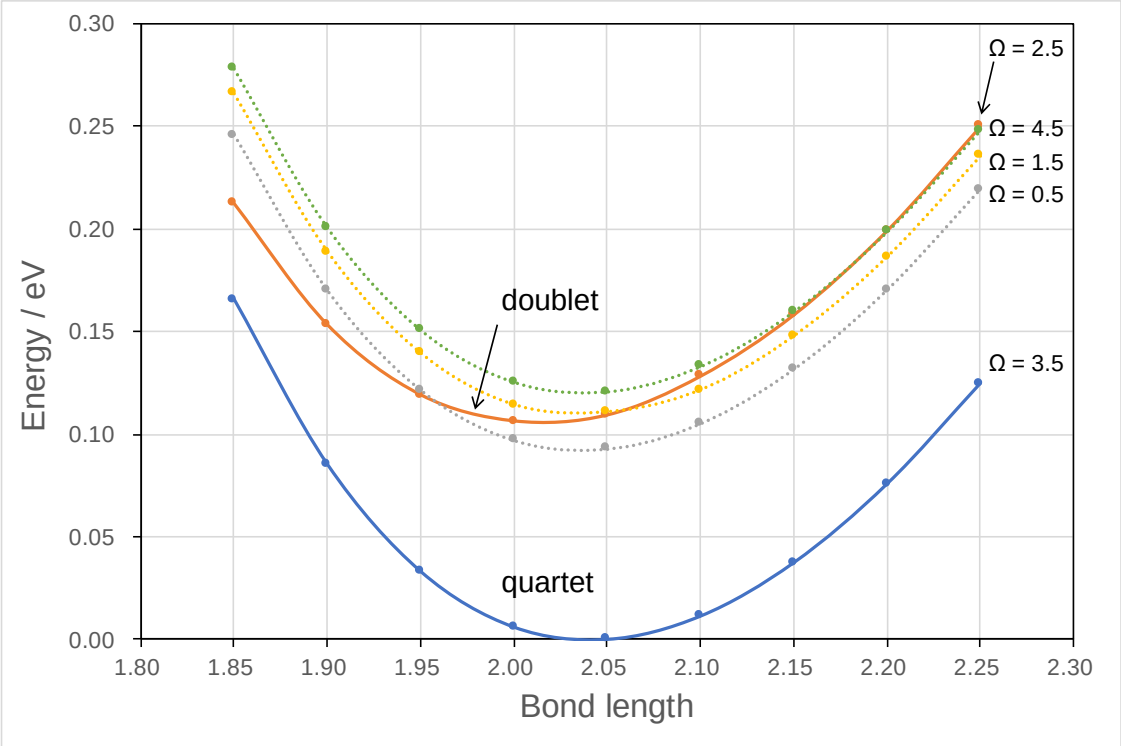

Figure 5-2. The potential energy curves of the low-lying five electronic states of CeH with Ω = 3.5, 0.5, 1.5, 4.5, and 2.5 where only the state with Ω = 2.5 has a contribution from doublet state, calculated by SA-CASSCF/NEVPT2+SOCI.

Then, I calculated the bond length (equilibrium and zero-point vibrational state) and frequency (harmonic and fundamental) for the lowest quartet (ground state, Ω = 3.5) and the lowest doublet (Ω = 2.5) states, by numerically solving the rovibrational Schrödinger equation using the MOLCAS program [18]. Table 5-1 summarizes the calculated bond lengths and stretching frequencies for CeH with the available experimental data [2]. The experimental Ce-H stretching frequency, 1271 cm^{-1}, is very

close to the calculated one for the quartet, 1291 cm^{-1}, which also support the ground state of CeH is quartet state.

Table 5-1. The bond length (equilibrium (r_e) and zero-point vibrational state (r_0)), and the vibrational frequency (harmonic one (v_e) and fundamental one (v_0)) of CeH for the lowest quartet state and doublet state, calculated at the SA-CASSCF/NEVPT2+SOCI level, with the available experimental data.

	r_e (Å)	r_0 (Å)	v_e (cm^{-1})	v_0 (cm^{-1})
quartet state (Ω = 3.5)	2.041	2.052	1390	1291
doublet state (Ω = 2.5)	2.017	2.020	1314	1229
Expt. [2]	–	–	–	1271

5.4 Conclusion

In this chapter, I employed SA-CASSCF/NEVPT2+SOCI approach with the Sapporo all-electron relativistic basis sets, to calculate the lowest-lying quartet and doublet states. As available experimental data, only Ce-H stretching frequency measured in matrix isolation spectroscopy was reported. Previous theoretical calculations could not determine whether the ground state of CeH is quartet or doublet since their energy difference is very small. The present state-of-the art *ab initio* all-electron calculations have clarified that the ground state of CeH is $^4H_{7/2}$, with the doublet state (Ω = 2.5) lying 0.1 eV high. The calculated Ce-H frequency in the $^4H_{7/2}$ state is in very good agreement with the experimental value, confirming our conclusion.

5.5 References

[1] M. Dolg and H. Stoll, Theor. Chim. Acta **75**, 369 (1989).

[2] S. P. Willson and L. Andrews, J. Phys. Chem. A **104**, 1640 (2000).

[3] E. Goto, Master Thesis in Hokkaido University (2009).

[4] H. Tatewaki and T. Koga, Chem. Phys. Lett. **328**, 473 (2000).

[5] M. Sekiya, T. Noro, Y. Osanai, E. Miyoshi, and T. Koga, J. Comput. Chem. **27**, 463 (2006).

[6] A. Wolf, M. Reiher, and B. A. Hess, J. Chem. Phys., **117**, 9215 (2002).

[7] MOLPRO, version 2006, a package of *ab initio* programs, H.-J. Werner, P. J. Knowles, R. Lindh, F. R. Manby, M. Schütz, P. Celani, T. Korona, A. Mitrushenkov, G. Rauhut, T. B. Adler, R. D. Amos, A. Bernhardsson, A. Berning, D. L. Cooper, M. J. O. Deegan, A. J. Dobbyn, F. Eckert, E. Goll, C. Hampel, G. Hetzer, T. Hrenar, G. Knizia, C. Köppl, Y. Liu, A. W. Lloyd, R. A. Mata, A. J. May, S. J. McNicholas, W. Meyer, M. E. Mura, A. Nicklaß, P. Palmieri, K. Pflüger, R. Pitzer, M. Reiher, U. Schumann, H. Stoll, A. J. Stone, R. Tarroni, T. Thorsteinsson, M. Wang, and A. Wolf.

[8] M. Sekiya, T. Noro, T. Koga, and T. Shimazaki, Theor. Chem. Acc., **131**, 1247 (2012).

[9] T. Noro, M. Sekiya, and T. Koga, Theor. Chem. Acc., **131**, 1124 (2012).

[10] T. Noro, Segmented GTF basis set factory, http://sapporo.center.ims.ac.jp/sapporo/ (accessed December 8, 2017).

[11] H.-J. Werner, P. J. Knowles, G. Knizia, F. R. Manby, and M. Schütz, Wiley Interdiscip. Rev. Comput. Mol. Sci., **2**, 242 (2012).

[12] MOLPRO, version 2012.1, a package of *ab initio* programs, H.-J. Werner, P. J. Knowles, G. Knizia, F. R. Manby, M. Schütz, P. Celani, T. Korona, R. Lindh, A. Mitrushenkov, G.

Rauhut, K. R. Shamasundar, T. B. Adler, R. D. Amos, A. Bernhardsson, A. Berning, D. L. Cooper, M. J. O. Deegan, A. J. Dobbyn, F. Eckert, E. Goll, C. Hampel, A. Hesselmann, G. Hetzer, T. Hrenar, G. Jansen, C. Köppl, Y. Liu, A. W. Lloyd, R. A. Mata, A. J. May, S. J. McNicholas, W. Meyer, M. E. Mura, A. Nicklass, D. P. O'Neill, P. Palmieri, D. Peng, K. Pflüger, R. Pitzer, M. Reiher, T. Shiozaki, H. Stoll, A. J. Stone, R. Tarroni, T. Thorsteinsson, and M. Wang, see http://www.molpro.net.

[13] J. Olsen, B. O. Roos, P. Jørgensen, and H. J. A. Jensen, J. Chem. Phys., **89**, 2185 (1988).

[14] C. Angeli, R. Cimiraglia, S. Evangelisti, T. Leininger, and J.-P. Malrieu, J. Chem. Phys., **114**, 10252 (2001).

[15] C. Angeli, R. Cimiraglia, and J. P. Malrieu, J. Chem. Phys., **117**, 9138 (2002).

[16] C. Angeli, M. Pastore, and R. Cimiraglia, Theor. Chem. Acc., **117**, 743 (2007).

[17] A. Berning, M. Schweizer, H.-J. Werner, P. J. Knowles, and P. Palmieri, Mol. Phys., **98**, 1823 (2000).

[18] F. Aquilante, L. De Vico, N. Ferré, G. Ghigo, P.-Å. Malmqvist, P. Neogrády, T. B. Pedersen, M. Pitoňák, M. Reiher, B. O. Roos, L. Serrano-Andrés, M. Urban, V. Veryazov, and R. Lindh, J. Comput. Chem., **31**, 224 (2010).

6. General Conclusion

The purpose of this dissertation is a challenge to the complex electronic structure system by a state-of-the art *ab initio* wavefunction theory. I worked on *ab initio* computations on the small molecular systems containing heavy atoms such as lanthanide element by employing highly-sophisticated electronic structure theories, considering both static and dynamic correlation effects, scalar and spin-orbit relativistic effects, and treating multiconfiguration-multistate features of the near-degenerate low-lying electronic states. In Chapter 1, I give a brief description of the background of a modern quantum chemical computation. The foundation of *ab initio* wavefunction approach is a choice of the many-electron wavefunction methods and the basis sets for a one-electron wavefunction; as for the many-electron wavefunction method, I employed a gold-standard approach in modern quantum chemistry, CCSD(T), and a multiconfigurational-multireference wavefunction, SA-CAS(RAS)SCF/NEVPT2, while as for the basis sets to describe the one-electron wavefunction, I employed the Sapporo basis sets which have been developed so that the electron correlation and relativistic effects are treated appropriately.

In Chapter 2, I formulated a procedure to calculate the spin-orbit coupled states by combining the CCSD(T) energies and SA-CASSCF spin-orbit coupling elements, and applied the procedure to the transition metal triatomic molecules, PtCN, PtNC, PdCN, and PdNC, to examine the electronic configuration in the ground state of the respective species. It was demonstrated that the spin-orbit coupling effects changed the lowest-lying electronic states of PtCN and PtNC from $^2\Sigma$ to $^2\Delta_{5/2}$. On the other hand, the electronic ground states of PdCN and PdNC remained to be $^2\Sigma_{1/2}$ even after considering spin-orbit

coupling effects. These calculations are in consistent with the spectroscopic experimental data, and the significance of spin-orbit interaction is shown clearly in these applications.

In Chapter 3, *ab initio* all-electron computations have been carried out for the lanthanide atom monovalent cation, Ce^+, including the electron correlation, scalar relativistic, and spin-orbit coupling effects in a quantitative manner. Following the computational scheme introduced in Chapter 2, the NEVPT2 and SOCI based on the SA-RAS(CAS)SCF wavefunctions have been applied to evaluations of the low-lying energy levels of Ce^+ with $[Xe]4f^15d^16s^1$ and $[Xe]4f^15d^2$ configurations, to test the accuracy of several all-electron relativistic basis sets. The numbers of the near-degenerate quartet states originating from the respective $[Xe]4f^15d^16s^1$ and $[Xe]4f^15d^2$ configurations are 140 and 280, showing a very crowded energy levels in a narrow energy region. To make the problem simpler, I first calculated the spin-orbit uncoupled states without SOCI, and compared the energy levels between theory and experiment. The dynamic correlation effect due to valence electrons and core electrons were discussed separately through a comparison of RAS(CAS)SCF and NEVPT2 results using several different basis sets (ECP and all-electron). It is shown that the mixing of quartet and doublet ensembles is essential to reproduce the excitation energies of Ce^+.

In Chapter 4, the same computational scheme as that for Ce^+ (SA-RAS(CAS)SCF/NEVPT2+SOCI with the Sapporo (-DKH3)-2012-QZP basis set) was employed to calculate the ground and low-lying excited states and spectroscopic constants of CeF. CeF is an ionic molecule between Ce^+ and F^-, and the near-degenerate 420 electronic states show splitting due to the bonding with F^-. It is interesting to note

that the ground-state ([Xe]$4f^1 5d^2$) and excited-state ([Xe]$4f^1 5d^1 6s^1$) configurations in Ce^+ are exchanged in CeF, which can be explained by the Coulomb repulsion from F^-. The effects of the mixing of doublet and quartet ensembles are discussed. The calculated excitation energies, bond length, and vibrational frequency are shown to be in good agreement with the available experimental data.

In Chapter 5, I carried out SA-CASSCF/NEVPT2+SOCI calculations with Sapporo basis set for CeH diatomic molecule, to investigate the electronic structure of the ground state, as well as to reproduce the Ce-H stretching frequency reported by the experiment. The difference between CeF and CeH is a covalent nature for CeH where the bonding orbital is made between Ce-$5d_\sigma$ and H-1s. The previous DFT and CCSD(T) calculations predicted the ground state of CeH to be doublet, while the present multireference perturbation theory including spin-orbit coupling effects lowers the quartet state extensively compared to the doublet state, resulting in that quartet becomes the ground state. The Ce-H stretching frequency is well reproduced, and now theoretical approach has solved the problem in CeH.

I believe that the present demonstration provides a standard theoretical approach for the spin-orbit coupled multiple states for the chemical compounds containing heavy elements such as lanthanide elements.

7. Acknowledgements

First, I would like to express my acknowledgements to all members that helped or supported me during my doctoral course. I have been taken a lot of help and support . Here, considering my first name, Yusuke (有輔), Yu (有) means existing and suke (輔) means helping or supporting, so I have lived a fortunate research life as my first name suggests. From now on, I keep in mind not to be helped or supported but to help or support the people in need, as my first name suggests. In the following, I leave some remarks particularly on those who I am owing to in my research.

I would like to represent my sincere gratitude to Prof. Tetsuya Taketsugu for the generous help to me. He is the exceptional mentor for me but I believe that I have been the most annoying doctoral student to him, so if possible, I would like to contribute to his Quantum Chemistry laboratory.

I am embedded to Prof. Takeshi Noro for teaching me the foundation of quantum chemistry. For the first year when I joined the QC lab, I participated in the seminars of reading the introductory textbook, Szabo, and I experienced deep thinking for the first time. This experience is the driving force for my research life.

I would like to express the deepest appreciation to Prof. Masato Kobayashi for managing the computational environment of QC laboratory and giving the sage advice for this study. To perform the electronic structure calculation for 420 states, He compiled MOLPO program and adjust the computational environment.

I would like to show my greatest appreciation to Prof. Satoshi Maeda. His advices and comments make me notice another perspective.

I would like to thank Prof. Takeshi Iwasa, for the discussion in weekly-based seminar. I respect his attitude to positively ask questions.

I would also like to thank Prof. Gao Min and Dr. Yuriko Ono. Their encouragement and advice about the research life and this study, I was able to complete my doctoral course. Here, I apologize to them for causing trouble.

Finally, I appreciate my parents and other families for allowing me to take the doctor's course. Without my family's supports, I could not complete this course. Thank you so much.